AN ABSTRACT OF THE THESIS OF

Ivan A. McCracken for the degree of Master of Science in Mechanical Engineering presented on April 25, 2003.

Title: Processing Bulk Metallic Glass from the Molten State

Abstract approved:

Ralf Busch

This paper documents the investigation into injection molding, or die casting, a bulk metallic glass (BMG). A BMG is an amorphous metal of a thickness greater than 25 μm, according to leading researchers in the field. This critical thickness differentiates a normal metallic glass from a "bulk" metallic glass. The impetus for studying the ability to process lies in the material properties of the BMG, which has twice the strength of steel and the ability to be formed much like a thermoplastic. An initial discussion of processing options and history precedes a detailed description of the machine concept and design, including the governing parameters placed on the design. An account of methods and materials used has been included, along with problems encountered and resultant remedies. The initial results consist of the verification of the machine concept and the ability to replicate nanometer-sized surface features from a mold. Design issues are addressed and the corresponding revisions described. The final machine revision shows an increase in process repeatability. A presentation of photographs, which show results of forming the BMG against both copper and stainless steel, is offered as a qualitative assessment of the processing capability. A discussion of considerations and paths forward has been included for future research using the machine that was developed, but these processing theories could also be carried over to other experiments. In the end, this study proves the ability to form extremely small surface features in cast BMG parts and makes suggestions on research avenues that may give a better understanding of the variables involved in processing BMG from the molten state.

Processing Bulk Metallic Glass from the Molten State

by
Ivan A. McCracken

A THESIS

submitted to
Oregon State University

in partial fulfillment of
the requirements for the
degree of

Master of Science

Presented April 25, 2003
Commencement June 2003

Master of Science thesis of Ivan A. McCracken presented on April 25, 2003.

APPROVED:

Redacted for Privacy

Major Professor, representing Mechanical Engineering

Redacted for Privacy

Head of the Department of Mechanical Engineering

Redacted for Privacy

Dean of the Graduate School

I understand that my thesis will become part of the permanent collection of Oregon State University libraries. My signature below authorizes release of my thesis to any reader upon request.

Redacted for Privacy

Ivan A. McCracken, Author

ACKNOWLEDGEMENTS

This project would not have happened without the generous project latitude given me by Dr. Ralf Busch. I would like to thank him for his straightforward and practical approach to management of the project and overall lab group. He acted as a consistent sounding board for me as well as a source for new ideas. My appreciation also goes out to Manfred Dietrich, best machinist this side of the Rockies, for his good insight and clever solutions. Tyler Shaw wrote the Labview© code that ran the machine, and I thank him for saving me a heap of frustration. I am also grateful to the lab groupies, who helped me through many a windowless summer day. Finally, I would like to thank Ludi Shaddowspearker; his mere presence awakens the mind and most always brings a smile!

TABLE OF CONTENTS

TABLE OF CONTENTS (Continued) Page

LIST OF FIGURES

LIST OF FIGURES (Continued)

LIST OF FIGURES (Continued)

(Edward Lorenz)

Dedicated to all of the Butterflies in my life, both big and small...

Jamie Keeney
Jason Lawhon
Adam
Kevin Bucholtz
Tom Spear
Dave Therasse
Tom Matuzzo
Keith Rocca
Renninger
Justin Gallo
Mrs. Bucci
Jeremy Ickes
Rick Scaletta
Mrs. Cylenica
Judy Spear
Ralf Busch
Mr. Conners
Rick Shimpeno
Lori Mayton
Bill Warnes
Janale Moore
Isabella Gallino
Jillian Moore
Tyler Shaw
Bonnie Luchart
Tim Presto
Jill Groner
Nicole Coy
Morgan Porzio
Eric Spear
Atsushi Hirokoba
Gordy Simpson
Paul Koch
Heidi Felix
Jason Hutchison
Dave Niderost
David Vinca
Joel Spital
Mike Saab
Dave Kolenda
Satoka Suzuki
Jerry Leonard
Edith De Santi
Mr. Jahn
Pamela Hamilton
Chris Daum
Jaynell Dean
Linda McCracken
Josh Bond
Todd Fytczyk
Stuart Edwards
Aaron Domes
Bill Johnson
Brian Deforce
Mike & Mary Niderost
Emily
O
E
W
Levi Kilcher
Allyson Cummings
Jason Hobbs
Corbin Murphy
Brandon Clark
Jesse Ogle
Denise Hollman
Keegan Mullaney
Mandy Danelson
Dave Vernor
Evangeline Thai
Daniel Schwartz
Angie Liesure
Mr. Korb
James Hyden

Clyde McCracken
Brendan Seonnecken
Chad Deforce
Mr. Donche
Ludi Shaddowspeaker
Betty & Clark Deforce
Bjorn Gumpas
161A Ligon Crew
Nate Slegers
Mike Kassner
Fred Ellsworth

Rueben Oder
Ben Gaw
Phil Kacerik
Mike Orr
Chad Perrin
Barb Renninger
Jonathan Carlson
Jeff Spires
Dan Calhoun
Lester McCracken
Sir Robert Jennings
Monica Grover
Joe Krupp
Andy Lamont
John Miller III
Gary
Ali Clow
Mike Kath
Jillian Moore
John Raybuck
Lance Mroz
Paul Doolan
Justin Steubs
Bobby Mitchell
Kristy Pocious
Amy Belling
Angela Jennings
Roger & Sandy Paul
evie
moe
Bastian Bayer
Judy Scaletta
Caroline Hilton
Sue Potter
Eric York
Matt York
Mary Deale
Jon Smyth
Kizzy Ellis
Wilson Parish
UCC
Heath Cloutier
Jesus Christ
Adams
Randy Stigall
Daniel Heuer
Tony Desaro
Al & Betty Karp
Dan Palcano
Bronwyn Giles
Duane Morris
Emelia Omniewski
Erin Tomcho
Todd Denlinger
John P. Beaumont
Prue Hill
Carl Kuester
Dave Sanders
Neil Paton
Josh Johnson
Ben Hokenson
Candice Kemp
Mr. Berlin
Mrs. Bozman
Lon Jenkins
Mr. Williams
Skip Rochefort
John Ralston
Joe & Luke
Abbie
Mrs. Wilson
Mr. Woodward
George Shimpeno
Mr. Smrekar
Trond Smallenberger
Aaron Watters
Doug Way

Processing Bulk Metallic Glass from the Molten State

1. INTRODUCTION

This work serves as a summation of initial investigations into the processing of bulk metallic glass (BMG) alloys. The primary goal of the project was to design and build a machine capable of forming a bulk metallic glass in a mold from the molten state. This machine would also provide a means to study the variables that affect the ability of the glass to reproduce surface features. Of particular interest was the feature size down to which the alloy is capable of replicating. Comments on the general processing characteristics of the alloy and, consequently, the efficacy of the machine in casting the alloy have also been included in this study.

1.1. Amorphous metals

1.1.1. General description

Before an explanation of the study can be appreciated, a clarification and definition of terms may be helpful for those unfamiliar with BMG alloys. A BMG may also be referred to as a vitreous alloy, or structural amorphous metal (SAM). "Bulk metallic glass" is the term most widely used, and it best describes the uniqueness of the alloy.

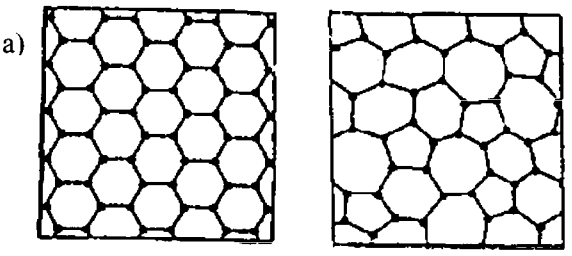

Figure 1. *Schematic representation of the (a) atomic arrangement of a crystalline and (b) amorphous solid.*

A metallic glass has no order at the atomic level; it is amorphous, like silicon oxide, commonly known as window glass. The atoms in a glass exist in a random arrangement relative to each other, not only in the liquid state, but also in the solid state. By rapidly removing heat from the melt, the atoms essentially freeze before moving into the lattice position of the crystalline equilibrium phases. This differentiates a metallic glass from all other metals and alloys, which have crystal structures, and, therefore, grains and grain boundaries (except single crystals). See Figure 1. The "bulk" in BMG refers to the critical thickness of the metallic glass, which, until recently, was on the order of micrometers. Now, specific alloying enables greater thickness for the metallic glass. Contemporary metallic glasses exist by controlling the roles that entropy, enthalpy and density take on as the melt cools. A discussion of these roles follows.

1.1.2. Specific definitions

For all intents and purposes, the BMG is a solid below its glass transition temperature (T_g). Because the alloy is amorphous, having no crystal structure, a softening, rather than melting, is said to occur upon heating. The glass transition defines the temperature (T_g) at which atomic motion begins or ceases in an amorphous material. T_g is dependent upon the heating, or cooling, rate and must therefore be reported as a temperature range, rather than a point constant. Specifically, T_g defines the temperature, during heating, at which the typical relaxation time (t_r) becomes shorter than the laboratory time. The relaxation time is temperature dependent and defines the time required for atoms to move into their respective metastable equilibrium locations, to achieve the lowest overall thermodynamic energy state for the amorphous material. Furthermore, the relaxation time is proportional to viscosity, which quantifies a liquid's resistance to flow. The importance of defining T_g, then, becomes apparent with respect to differentiation between the liquid and solid states of the BMG. It is generally accepted that a viscosity greater than 10^{12} Pa-s denotes a solid. The critical cooling rate defines the rate of heat removal which forces the metallic alloy to remain amorphous. If heat is not removed at this rate (or faster), the metal will crystallize. The critical thickness (x_{cr}) is defined by $x_{cr} \propto \sqrt{(2h^*t_{cr})}$, where h is the thermal conductivity and t_{cr} is the critical cooling time. According to this relationship, the thickness is proportional to the square root of the cooling time. It follows, then, that if the critical cooling time of the material is reduced by a factor of 10^6, the thickness of the material may increase by a factor of 10^3 and the material will remain amorphous. This corresponds to the improvement of critical thickness from about 25 μm in conventional metallic glasses to 25 mm in bulk metallic glasses.

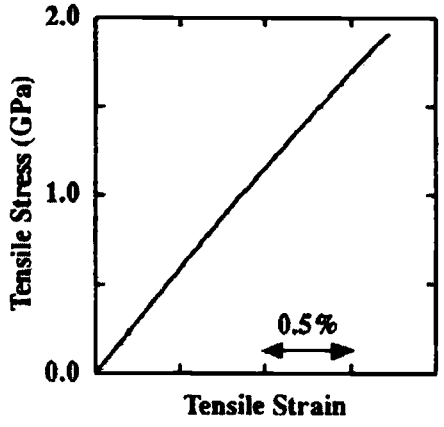

Figure 2. *Stress-strain plot*[1] *for Vitreloy 1* ™ [$Zr_{41.24}Ti_{13.75}Cu_{12.5}Ni_{10}Be_{22.5}$]

1.1.3. Material Properties

The random atomic nature of the BMG results in unique material properties. All crystalline materials have dislocations, which are the vehicles for plastic deformation. This results in a decrease of strength for the material, as compared to the theoretical strength. The metal relies on pinning of dislocations to increase the yield and ultimate strength. Because no crystal

structure exists in a BMG, grain boundaries and dislocations are also absent. It follows, then, that the strength of the BMG comes directly from atomic bonding strength. The BMG strength, therefore, is closer to the theoretical maximum strength. Plastic deformation occurs in shear bands less than 45° to the direction of applied force. In tension, the material fails catastrophically with one single shear band. In compression, multiple shear bands form, leading to yielding and plastic flow without strain hardening. Figure 2 shows a tensile stress-strain plot for the BMG glass used in this study. Table 1 is a compilation of some of the common material properties for the BMG.

Table 1. *Physical Properties of Vitreloy 1 ™* [$Zr_{41.24}Ti_{13.75}Cu_{12.5}Ni_{10}Be_{22.5}$].

Elastic Modulus [GPa]	96
Tensile strength [MPa]	1900
Poisson's ratio	0.36
Bending Strength [GPa]	3.2
Shear Modulus [GPa]	34.3
Vickers Hardness [kg/mm^2]	534
Rockwell "C" scale hardness	51
Strain-to-failure (tension) %	2
Plane-strain fracture toughness, KIC, [MPa-m^1/2]	~55
Resistivity, [mOhm-cm]	190
Thermal Conductivity [W/m-K]	3.5
Coefficient of Thermal Expansion [ppm/°C]	8.5
Specific Heat (at constant pressure) [J/(g-at.-K)]	27@ 300K
	30@600K
	47@700K
Density [g/cm^3]	~5.9
Atomic weight	60
Total Hemispherical Emissivity	0.22@980K
	0.18@670K

1.2. Historical Overview: Processing Bulk Metallic Glasses

In 1960 Duwez used Au_3Si to form the first metallic glass from the melt state by achieving cooling rates of 10^6 K/s using a splat quenching technique[2]. Drehman, Greer, Kui, and Turnbull worked on the first bulk metallic glass in 1984, which was a Ni-Pd-P alloy with a critical cooling rate of ~10 K/s.[3,4] In 1985, Schwarz and coworkers used laser quenching to create nano-thick

glassy layers of Nb-Ni.[5] Vitreloy 1™ was the first (and currently is the only) commercially available BMG. A. Peker and W.L. Johnson developed Vitreloy 1™ at Caltech in 1992. This material was patented[6] in 1994 and is currently the property of Liquid Metal Technologies of Laguna Nigel, CA. Johnson reports the thickness of this BMG can be as great as 5 to 10 cm, the result of critical cooling rates on the order of 1-K/s.[7] Few studies have been carried out on the casting of bulk metallic glasses. That which has been done, has been concerned primarily with validating the critical thickness of a specific BMG composition. Inoue, and those working with him, used a casting process to do just this in the early 1990s.[8] Beginning in 1998, Vitreloy 1™ was processed commercially by the Howmet Corporation, Whitehall, MI, for Liquid Metal Golf Inc., Laguna Nigel, CA.[9] This latter company has since expanded its operations and changed names to Liquidmetal Technologies. They are currently manufacturing the alloy, Vitreloy 1™, and manufacturing BMG parts. But, their operations are proprietary, and for good reason. The obstacles in producing BMG parts are mated closely with the material composition, on which they have several patents. Most recently, J. Schroers and coworkers have created metallic foams using BMG.[10]

Most of the research in the area of BMG occurs in the area of material science. As with any material, the chemical composition drives the processing capability, and due to the relatively new nature of bulk metallic glasses, very few laboratories are equipped to deal with both the production of the alloy and the subsequent processing. One such laboratory exists at the California Institute of Technology, headed by Johnson. Successful molding of a BMG has been accomplished there on a laboratory scale. In their process; a quartz tube is melted at one end to form a rounded nozzle, which is pressed against the mold. The BMG sample is heated in the quartz tube, and the back end of the tube is attached to a hose, which allows compressed gas through during the injection stage of the molding. The mold is placed inside of a vacuum chamber, and the BMG shot sample (inside the quartz tube) is heated inside of the chamber by an induction coil. The back end of the quartz tube is attached to the hose, which is connected to a fluid feed through. The operator heats the sample up to a certain level of brightness (approximation of temperature), which is determined by the operator through experience. At this point, the operator opens a valve, which breaks the vacuum above the melt and allows the compressed argon to force the melt into the mold.

2. MACHINE DESIGN

2.1. Existing Machines

Processing metals from a molten state is a common practice, the most primitive of which is casting. The casting process eliminates forming time by producing a metal part at or near the final shape. Die-casting, specifically, allows for the forming of parts with tighter tolerances, often without the need for further machining. In die-casting, the liquid melt is forced into the mold at a high pressure, which corresponds to the high velocity needed to push the molten metal into the mold before it cools. The plunger acts to both force the metal into the mold and apply a holding pressure, which pushes the melt onto the mold walls and prevents backflow. Smoother surface finish is one benefit die-casting provides over conventional casting. Vacuum die-casting enables a melt to be processed in a controlled environment, i.e. oxygen free. Bulk metallic glasses must be processed in such an environment to avoid crystallization. In order to produce cast parts with microscopic surface features, then, a vacuum die-casting machine would seem to be the system design of choice. There exist, however, several reasons not to use an existing machine to study process capability, which will be addressed in the following section.

2.2. Justification for Original Machine Design

It would have been possible to retrofit an existing vacuum die-casting machine to obtain the information desired in this study; but the largest governing factor in this study was cost, which, at the university level, should come as no surprise. Besides having insufficient funds to purchase an existing machine, the size of such a machine prevents it from being practical. The footprint of a small machine[11] averages 2.8 m^2 [30 ft^2], not including the space required for vacuum and cooling equipment. The barrel, or pot in the case of hot chamber die-casting, and plunger head are made of metal, and a BMG is highly reactive in the molten state; see the next section on machine requirements. The major obstacle, however, was shot size. This reached a low at around 250 grams for a commercial machine. Because new BMG alloys will not be readily available, the cost of the material is prohibitive. The difficulties associated with producing the material require the amount of material waste and shot size to be kept to a minimum. The sprue from a die-casting machine would be many times the weight of the cast part necessary to collect data on surface features, as cast samples needs to be only a few grams for the study. Furthermore, new alloys will be formulated in small batches, and it will be necessary to study their processing capabilities as well. BMG samples are produced in a laboratory using either a water-cooled

copper (or silver) boat, or an arc melting system. The average batch size is approximately ten grams.

2.3. Requirements of Machine

Let us now consider the requirements for casting a bulk metallic glass. The BMG, above its glass transition temperature, will react with almost anything. The reactivity, however, like most elements, is a function of time and temperature. The materials, which come into direct contact with the melt, must therefore be chosen as to minimize the amount of reaction at the contact surfaces. A mold is required to shape and cool the melt, as well as provide features for the BMG to replicate. There must be a way of heating the BMG to a molten state. A melt delivery system must then transport the BMG from where it is heated to the mold cavity. These systems must be designed to handle a small shot size as earlier discussed. To avoid oxidation, there must be a way to apply a high vacuum to any area in which the BMG will be molten. The temperature of the mold must be controlled. The temperature of the melt also needs to be measured before entering into the mold. Both measurements must be reproducible for data collection purposes. The machine must be adaptable to allow for varying mold designs and shot sizes. The machine should also be easy to use and achieve the processing goals, which relate to surface replication.

2.4. Design to Meet Requirements

2.4.1. Reactivity

The materials, which were chosen to have contact with the molten BMG, were carbon,[12] fused quartz,[13] and oxygen-free-high-conductivity (OFHC) copper.[14] Fused quartz was chosen because it reacts slowly with the molten BMG. Quartz also has several other qualities, which were required of the design and made it suitable material for use as the injection barrel. It is available in standard sizes at high tolerances and in a competitive market, which keeps the price low, as each casting requires a new barrel. Other non-reactive oxides and ceramics are not readily available, require custom ordering, and are much more expensive. Carbon tubes would have also required expensive custom orders. Furthermore, there was the issue of transmissivity, which will be addressed in the melt temperature section (2.4.7). Quartz also displayed excellent thermal shock resistance, and has a softening temperature of 1670°C. The quartz tube could withstand a temperature gradient of 1000°C over one half an inch and not fail. Because of its low reactivity, carbon was chosen to fill a different role, which is addressed in the melt delivery section (2.4.4). Incidentally, carbon displayed the lowest reactivity with BMG throughout the study. The final

material, which had contact with the melt, was oxygen-free copper. The mold was made out of copper, the mass of which acted as a heat sink for the melt, allowing rapid cooling and preventing any reaction between the molten BMG and mold.

2.4.2. Mold Design

Of all the elements, copper is second only to silver in thermal conductivity. OFHC copper was chosen as the mold material for this reason. The mold cavity was machined with a tapered gate region to reduce pressure losses during injection, and the gate was placed at the thick end of the cavity so the melt flowed from a thick to thin in cross-section. The idea was to minimize the chance of freeze-off before fill. The transition between the two regions was smooth, again to minimize pressure loss and promote flow. The size of the cavity was small, for reasons discussed earlier, having a volume of 1.192 cm^3. The cavity dimensions were 3.18 x 12.70 x 19.05 mm (thick region) and 1.59 x 12.70 x 0.19.05 mm (thin region). The cavity size was dependent upon volume requirements of the heating system (see section 3.1). The method of heating the BMG, containment of the melt, and delivery of the melt into the cavity all played a role in determining the shot size. This will be discussed in section 2.4.4. The mold was a typical split mold, held together by five bolts, which thread into the cavity side of the mold. The bolts were used to provide a tight seal between the two mold halves, to prevent melt flash along the parting line. The gate entered the cavity along the parting line of the mold to simplify the ejection of the molded sample. Push-out (ejector) pins were avoided, as the frozen material in the gate region was to be used to pull the sample out of the cavity, which had a three-degree draft on the sidewalls to facilitate in mold release. Two bolts opposing the five clamp bolts were included to aid in opening the mold in the event that the BMG adhered to the mold and inhibited parting. Two guide pins were added to ensure the cylindrical

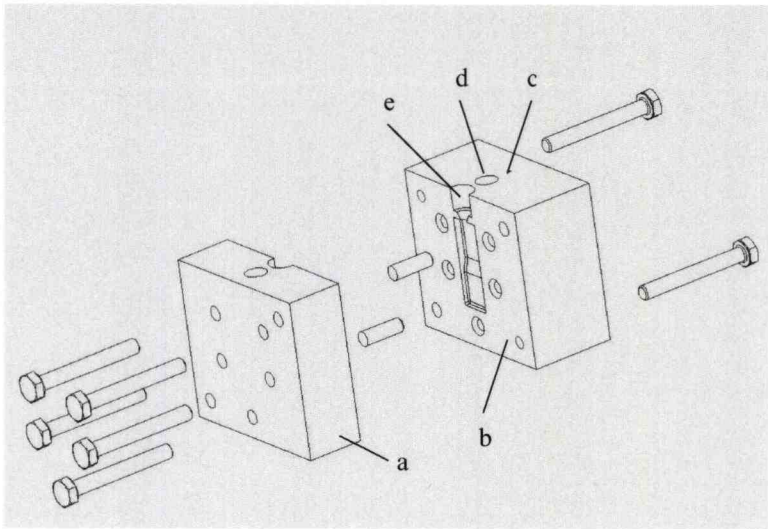

Figure 3. *Copper mold: (a) flat side, (b) cavity side, (c) slot for RTD, (d) slot for heater, and (e) barrel-mold interface.*

opening to the gate had precise alignment, allowing for a tight fit with the injection barrel. Figure 3 shows the mold design.

2.4.3. Heating the BMG

Due to the highly reactive nature of the BMG, it was necessary to heat the BMG to the injection temperature as quickly as possible. Reaction with the quartz would introduce contaminants and provide nucleation points for crystallization, preventing glass formation. An inductive heating machine[15] transfers heat to a specific area via electromagnetic waves, thus it is a non-contact means of applying heat. Copper tubing, shaped as a helical coil, extends out from the machine and wraps around the sample to be heated. The height of the coil determines the amount of BMG that can be heated, and this should be kept small to minimize the area of contact with the melt. The heat, applied to the sample, scales with the applied voltage. This means the BMG can be brought rapidly to the desired temperature. See Figure 4.

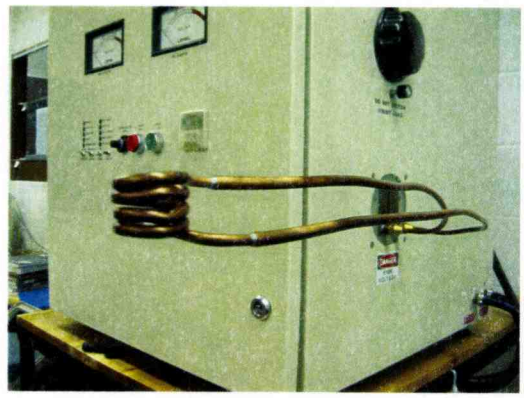

Figure 4. *Picture of induction heating machine and RF coil.*

2.4.4. Melt Delivery System

A melt-delivery system consists of two primary parts: the holding area for the material and the actuator. In the case of traditional casting, the holding area is the crucible, and the actuator is gravity and whatever tips the crucible. Similarly, in die-casting, there is the melt pool, which contains material for many castings, and the plunger, which acts on the melt pool. The early plastics injection molding machines incorporated a heated barrel and a hydraulic plunger. The plunger head was in direct contact with the melt and pushed from the back of the melt pool, through the barrel, and forced the entire barrel content into the mold cavity. The design for the BMG injection system has been modeled after this approach to injection. The plunger was used because it could provide a holding pressure on the melt as it solidified in the cavity. The holding pressure is intended to promote wetting between the BMG and mold surface, reproducing the fine features that may otherwise not fill due to the surface tension of the melt. This approach to injection requires the injection system be aligned vertically rather than horizontally, otherwise the melt will flow out of the heat region during heating. To avoid the need for a shut-off valve

between the melt and the mold, the injection system is positioned below the mold, so that gravity prevents the melt from prematurely entering the mold. The plunger, then, pushes the melt to the mold from below. This system is shown in Figures 5 and 6.

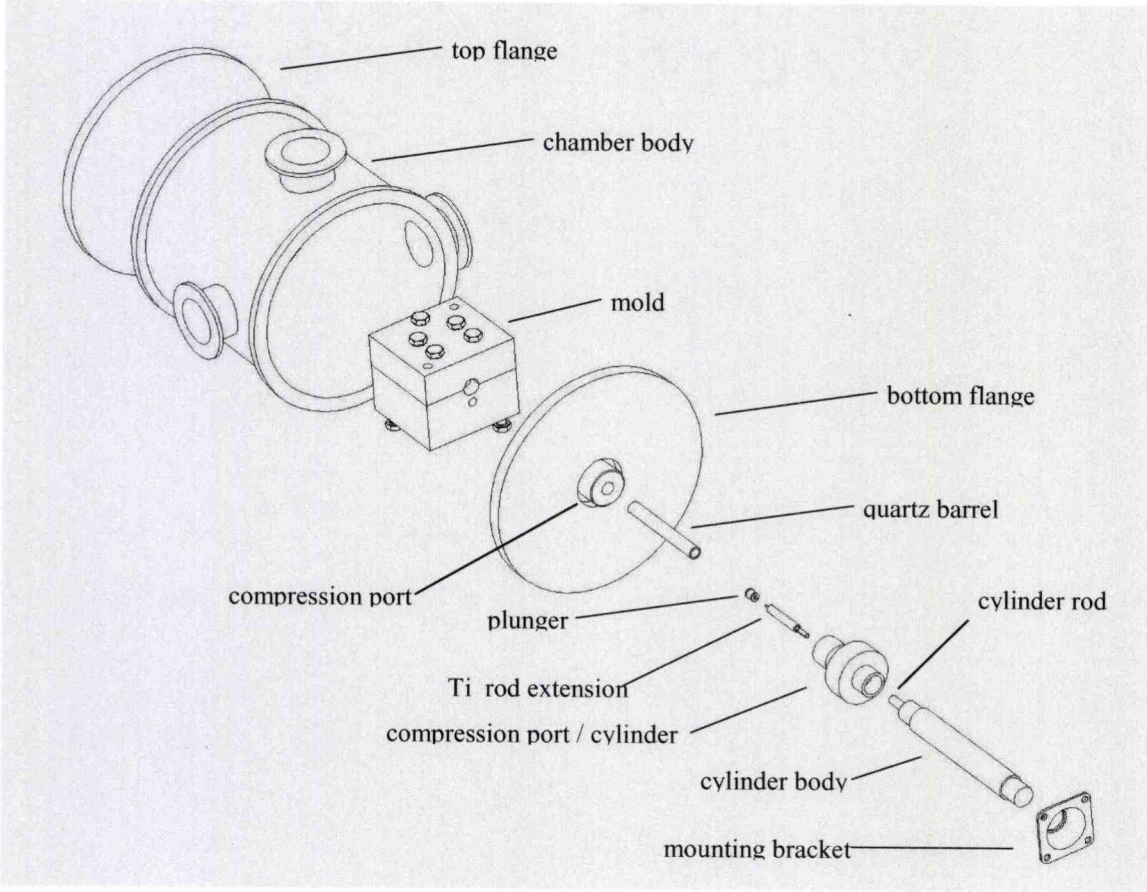

Figure 5. *Schematic view of the Injection assembly.*

2.4.4.1. Barrel

There are several attributes of fused quartz tubing that make it an ideal material for this application. Because the quartz tube is electrically nonconductive, the IR coil does not heat the quartz directly. As the BMG increases in temperature, it will heat the quartz through conduction, but the softening temperature of the quartz is around 1600°C and well above the operating temperatures of the system. The thermal expansion of the quartz is extremely low, 5.5×10^{-7} mm/°C, which allows for a constant fit between the quartz and the mold. The thermal conductivity is also low, approximately 1.9 $(J \cdot kg) \cdot m/(m^2 \cdot s \cdot °C)$, which helps isolate the heat in the area where the melt directly touches the quartz. Viton seals, needed for the vacuum, contact the

quartz one inch above and below the location of the shot (melt). The low thermal conductivity of the quartz prevents these from reaching the decomposition temperature for Viton, around 150°C. Most importantly, the fused quartz tube, transmits both visible and infrared (IR) light. This property enables the temperature of the melt to be quickly and accurately measured with an infrared thermocouple, discussed in section 2.4.7. Having an optically transparent barrel is also valuable for observing what happens during the heating and injection processes.

2.4.4.2. Plunger Head

The plunger head was made from a dense, semiconductor-grade, graphite. Besides having low melt reactivity, the plunger needed to be made of a material that had the ability to be machined, or had the ability to be modified in design and sized for thermal expansion. Furthermore, the coefficient of friction between the plunger and the quartz tube needed to be low in order to avoid seizing during injection. The graphite has these properties. Additionally, the matte black surface of the graphite acts as a near black body, which enables accurate infrared temperature measurement, discussed further in the section on melt temperature (2.4.7).

2.4.4.3. Actuator

A double-acting air cylinder[16] was modified by replacing the standard seals with Viton seals. This cylinder was chosen because it could be disassembled, cleaned, and re-lubricated with vacuum grease, which was necessary because a vacuum seal had to exist between the injection system and the outside atmosphere. The cylinder was tested for vacuum to 10^{-5} mbar. The seal at the nose of the cylinder, where the piston rod slides out of the chamber body, is the vacuum seal at back of the injection barrel. See Figure 6(b). The cylinder is rated to 1.7 MPa [250 psi], leaving the system flexible to accommodate various injection pressures.

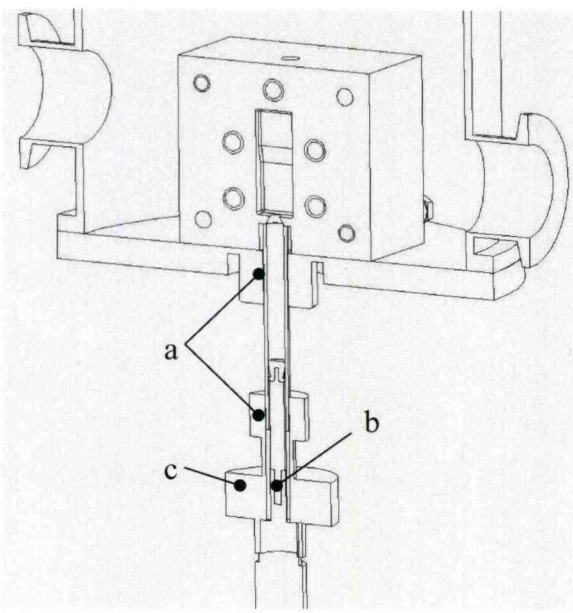

Figure 6. *Cross-section of injection system showing vacuum seal locations for the (a) barrel, (b) cylinder rod, and (c) cylinder body.*

2.4.4.4. Extension Rod

The plunger head is supported by a titanium shaft extension, which threads into the cylinder rod as an extension. See Figure 5. It was unknown how hot the rod would get, so titanium was used because of its high melting temperature. The plunger head has a slot fit to the titanium shaft. The extension distances the seal at the head of the cylinder from the RF coil, and it also distances the metallic components of the cylinder, which could couple with the RF coil.

2.4.4.5. Actuator Platform

The cylinder is mounted at the bottom to a stage that has horizontal movement along one axis. The stage and track are mounted on a platform. Four brass bushings and setscrews enable the platform to be raised and lowered along the four support columns. The platform can be raised to a height, which brings the top of the carbon plunger just below the bottom of the quartz barrel, and then fixed at this position. The cylinder can then be moved out of the way, along the stage

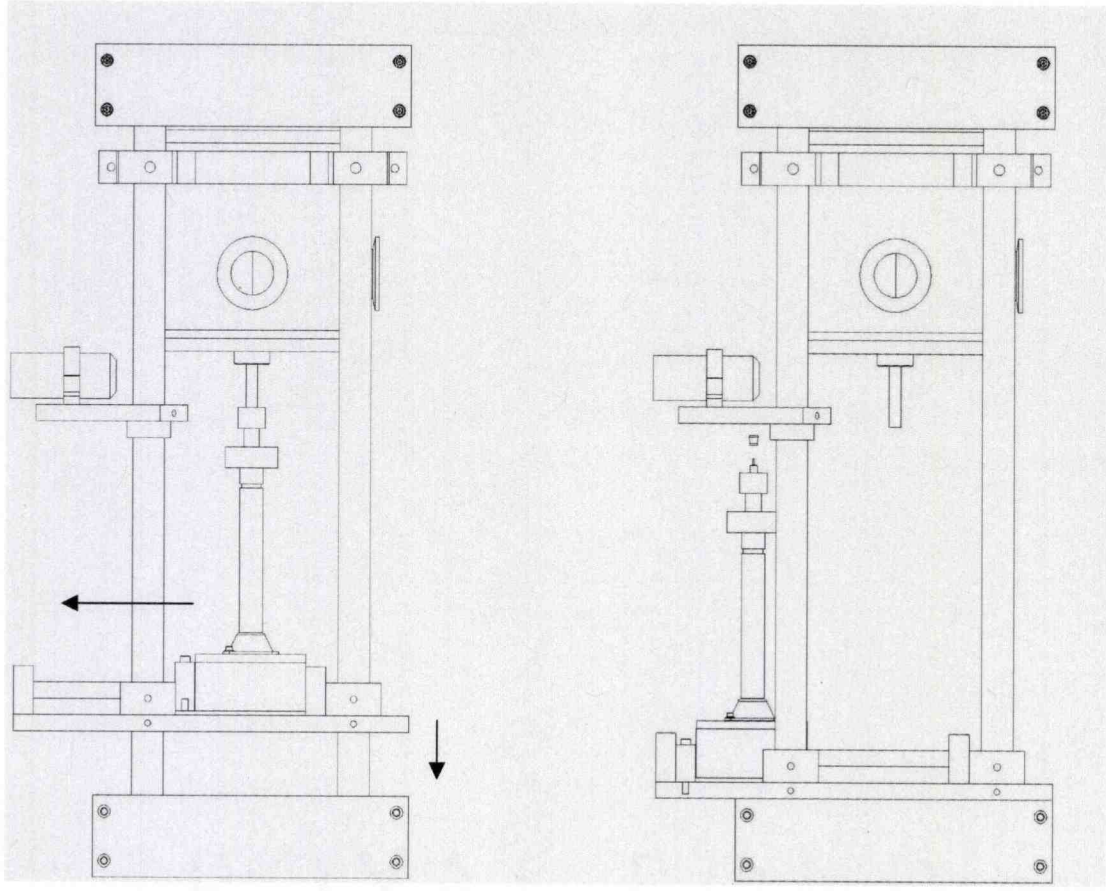

Figure 7. *Schematic side view of machine showing movement for loading of BMG.*

track, to load the sample, and then moved back into place so that the sample rests on the plunger inside of the barrel. The platform can then be raised to its final position and the compression fitting tightened between the cylinder and the barrel. This provides an easy method for loading the BMG sample into the barrel, as seen in Figure 7 above.

2.4.4.6. Inline Valves

The cylinder is driven by pressurized Argon in case any of the gas escapes past the seal. A two-way solenoid valve[17], normally closed, controls the flow of gas to the cylinder. Also inline is a manually controlled flow restriction valve, used to vary the speed and pressure at which the cylinder extends. The solenoid valve is powered by a 24V power supply,[18] and a computer-controlled switch is used to open and close the circuit. The valve-control setup can be seen to the right in Figure 8.

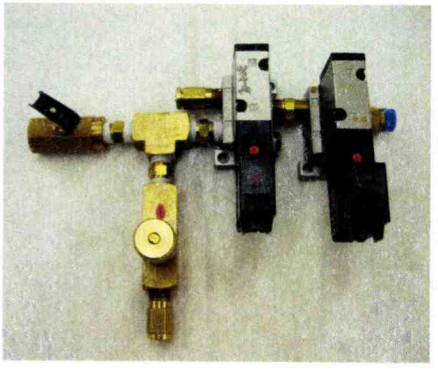

Figure 8. *Picture of inline valves and flow regulator.*

2.4.5. Vacuum Chamber

Several requirements of the study helped determine the design of the vacuum chamber, namely: cost, a need to measure the melt temperature, and the ability to adapt to future studies. By locating the melt delivery system outside the chamber, the cost was greatly reduced. The size of the chamber could be kept small enough to house only the mold. Vacuum feed-through ports were avoided for high-voltage RF (induction heater) and gas (injection cylinder). A sight glass for IR measurement was not needed. Staging fixtures for the mold placement and a chamber door were also designed out in order to keep costs low. In the end, keeping the injection system outside of the chamber resulted in a substantial cost reduction. An assembly of the machine, showing the location of the chamber can be found in Figure 9 on the following page.

2.4.5.1. Specific Requirements and Design of the Vacuum Chamber

To minimize the amount of custom welding and machining, the chamber was designed with standard parts, which were then customized and joined together. The main body of the chamber is a standard stainless steel cylinder, six inches in diameter and cut to a length of six inches. These dimensions allow for future testing variation, e.g. larger molds and other instrumentation.

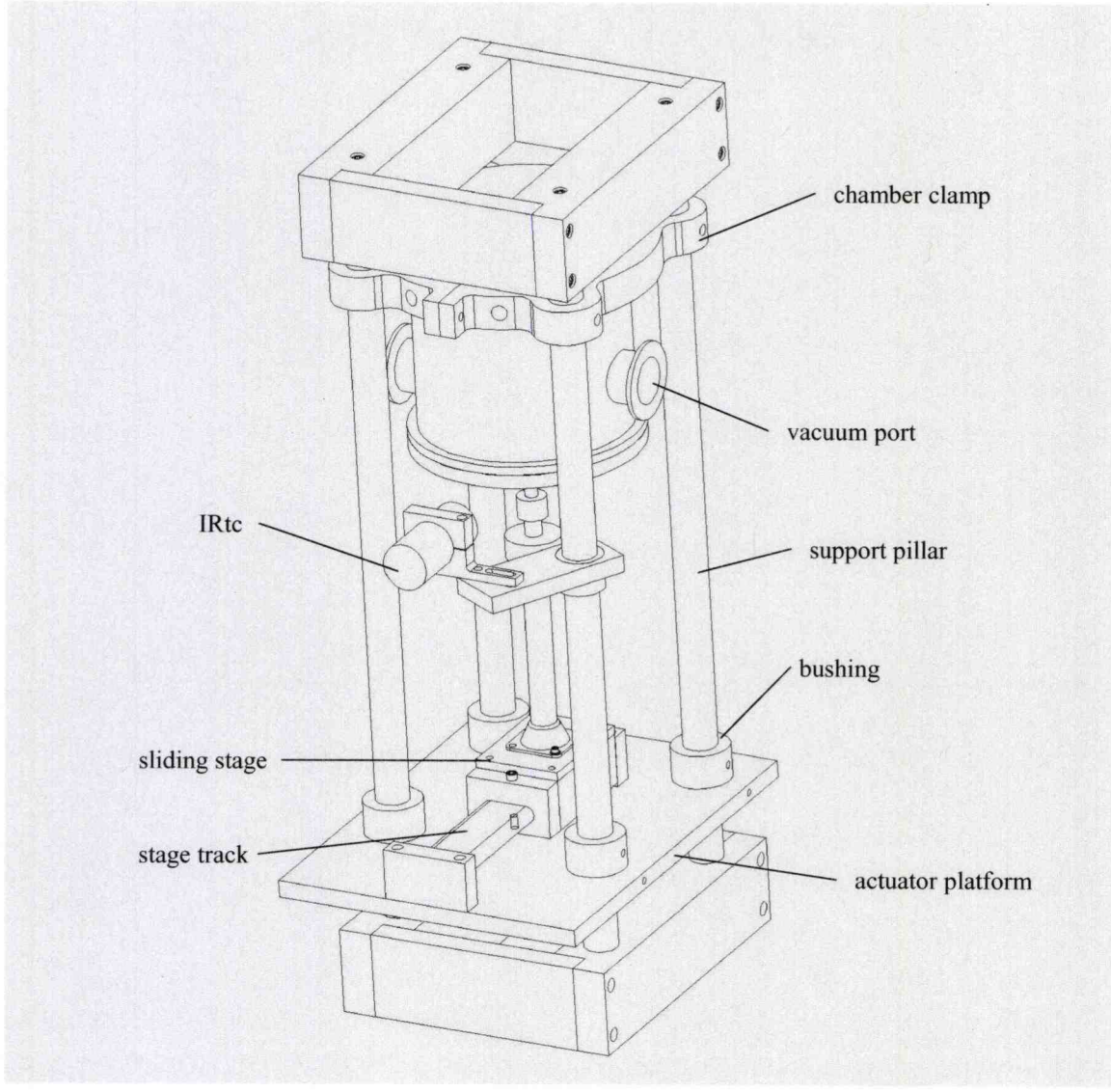

Figure 9. *Schematic view of the Machine assembly.*

Three ports were welded onto this cylinder: one for attachment to the vacuum system, and two others for instrumentation feed through. Clamp-on flanges with Viton seals used to seal the top and the bottom of the chamber. The bottom flange was modified by adding a screw-down compression port, which can best be seen in Figure 6. The quartz tube has a slot fit through this opening into the chamber and seated against the gate at the bottom of the mold. The distance the melt travels, from the heating area to the mold gate, had to be kept to a minimum. This is important to curtail heat loss, and the subsequent viscosity increase, which would occur during the travel of the melt from the heat zone. The shorter the distance between the top of the melt

shot and the back of the cavity, the less time the melt has to increase in viscosity during injection. The mold rests on the bottom plate of the chamber, and is held in place by a support column, which fits into the top of the mold. A downward force is applied to the top of the column by a spring attached to the top plate of the chamber.

2.4.6. Mold Temperature

Cartridge heaters are used to heat the mold. These are standard cartridge heaters, composed of wound nickel-chromium wire, swaged into a stainless steel cartridge with magnesium oxide. An electrical feed-through is attached to one of the ports. This serves to pass electricity from a power source[19] to the heaters and provided a feed through for a ceramic resistance temperature detector (RTD). An RTD uses resistance to measure temperature, and a hole was drilled for the cylindrical RTD to fit into the mold. To best measure the temperature of the mold cavity surface, the distance from the heater to the RTD is equal to the separation of the heater and cavity. The resistance is measured using a multimeter. Bare copper wires, separated by ceramic insulators, are used inside the chamber to connect the RTD and heaters to the feed through wires. The connection points are slot fit couplers, also copper. A picture of this setup is shown below in Figure 10. The heaters are capable of heating the mold to a temperature of 300°C in

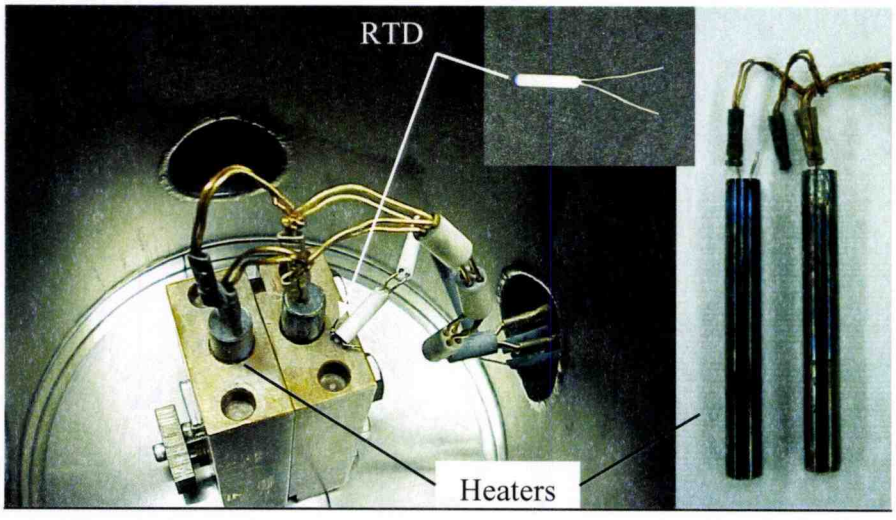

Figure 10. *Picture of cartridge heaters, RTD, and placement inside of the vacuum chamber.*

approximately fifteen minutes. An eighth-inch fused quartz plate is placed between the bottom of the mold and the bottom flange of the chamber. The quartz serves as an insulator to minimize the heat transfer from the mold to the chamber, and more specifically, to the vacuum seal located at the interface of the quartz barrel and the bottom of the chamber.

2.4.7. Melt Temperature

A temperature measurement device with a fast response time and low reactivity with the melt was required. An infrared thermocouple (IRtc) was chosen[20] in an effort to avoid designing a new type of thermocouple that would enable measurement in situ, as no existing thermocouple could meet the requirements. The IRtc measures the wavelength of light emitted from the melt and converts it to a voltage output, like a traditional thermocouple. The mV output corresponds to a temperature, which can be determined by calibration of the IRtc. This is discussed in the section 2.5. The response time of the thermocouple is 1/100 second, but this is reduced to 1/20 second by the hardware used in controlling the injection process. This is discussed in the following section. Response time is an important consideration because of the fast heating times required. The critical parameters for determining which IRtc to use were spot size, focal length, and emissivity range. The spot size requirement was predicated on the inside diameter of the quartz barrel, which was 7 mm. The focal length would determine the position of the instrument on the machine. It was necessary to be at least two inches from the RF coil, but not so far away as to require a separate stand for holding the IRtc. The model chosen has a spot size of 3.5 mm at a focal length of 104 mm, enabling it to be attached directly to the machine. The IRtc was specified to read wavelengths in the range from 0.1 to 5 μm. The quartz barrel allows infrared light up to a 3.5 μm wavelength to pass through with an efficiency of approximately 90 percent; see Figure 11. Specifying the IRtc to read as little of the background light as possible reduces the noise in the measurement system. The IRtc is shielded by a metallic housing, which, when grounded, protects it from interference caused by the RF heating coil. Direct contact with the melt results in either the corrosion of the probe or a reactive layer forming around it. This would prohibit reuse of the probe and would require its replacement in order to achieve reproducibility in a study. Altering the design of the machine would allow for the use of

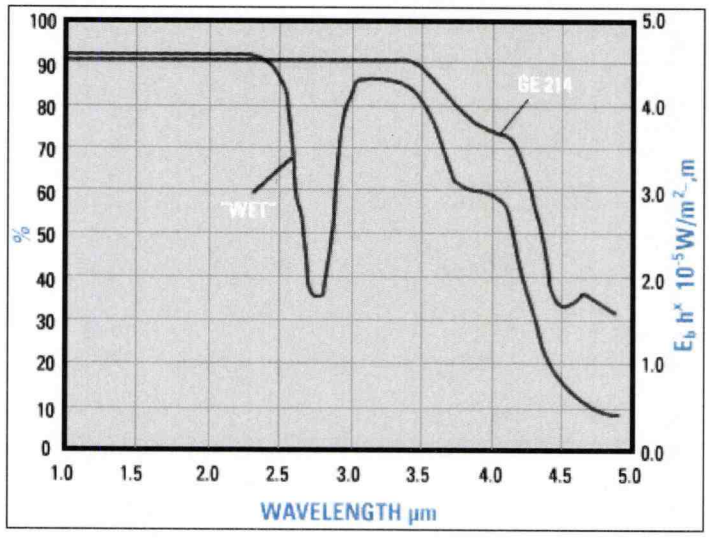

Figure 11. *Plot of IR transmission through quartz barrel: GE type 214.*[21] *"Wet" refers to quartz with a greater concentration of* OH^-.

contact probes, but this would not be a direct contact with the melt. Some other options are discussed later in chapter 7. Such options, however, were decided against at the outset due to the machine requirements listed above, namely cost and material selection.

2.4.8. Reproducibility

In an effort to minimize variation in data collection, a computer program was written to control the injection system. This program could monitor the temperature of the melt and was set to trigger the inline valve once the melt achieved that temperature. This program was also capable of controlling the power output of the RF coil, but this was not utilized during the study. The accuracy of the IRtc will be discussed in the section on IRtc calibration. One of the advantages to using an IRtc is its precision. Even if the measured temperature is not strictly accurate, due to a linear approximation, the reading is extremely reproducible. The accuracy of the RTD was specified as +/- 5% , and the accuracy of the multimeter used to read the resistance was +/- 1%. That combined to give an overall accuracy of +/- 15°C on average. The gauge on the pressure tank and an in-line flow restriction valve controlled the injection speed.

2.5. Calibration of Infrared Thermocouple

2.5.1. Procedures and Theory

Standard calibration of a thermocouple is relatively straightforward. A black body is raised to a given temperature, held at that temperature, and the output (mV) of the thermocouple is recorded. Because the relationship between temperature and thermocouple output is not linear, this is repeated for several temperatures over the desired measurement range. Over a small temperature range, however, the relationship can be approximated as linear, so that the distance between calibration points can be 100 degrees. The temperature of an object, then, may be measured by scaling the output of the thermocouple by that object's emissivity. This is providing, of course, that the emissivity is known, and the emissivity remains constant during measurement. In the case of the BMG, it would be possible to determine the emissivity, but that emissivity changes as the BMG forms a reactive layer with the material holding it (quartz in this case). For this reason, it was necessary to calibrate the IRtc in situ. Then, even if the emissivity changed, one could determine if it were changing in a reproducible manner. To test this theory, the reference temperature would be measured using a standard, pre-calibrated, thermocouple.

Three calibration scenarios are possible, each differing with the placement of IRtc and thermocouple. In one case, the IRtc is aimed at the melt, and the thermocouple is embedded in

the carbon plunger, 0.010" below the surface touching the melt. Case two has the thermocouple at the same location, but the IRtc is also aimed at the carbon, directly below the melt. Case three has the thermocouple protruding 0.005" past the carbon surface and into the melt and the IRtc aimed at the melt. A coil was made and bent with an opening that allowed for the IRtc sensor to "see" through the coil opening; refer to Figure 12. It was unknown if the tip of the thermocouple would survive the corrosive environment of the melt and report useable data, but this setup would provide the most robust measurement if so. This calibration was complicated because the BMG cannot be raised to the desired temperature and stabilized there. The certainty of calibration was to be determined by reproducing the curve created by plotting thermocouple versus IRtc output.

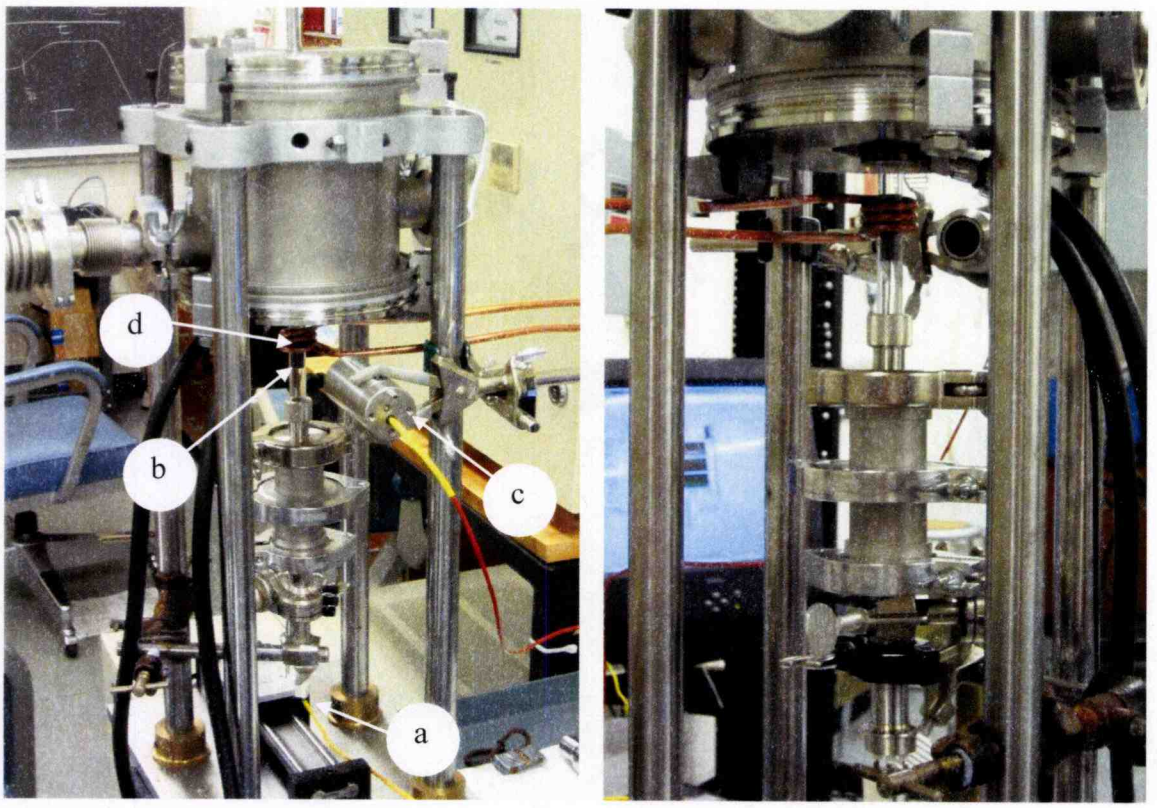

Figure 12. *Picture showing the calibration test setup. The components include the (a) thermocouple feedthrough, (b) thermocouple imbedded in carbon inside of the quartz barrel, (c) IRtc, and (d) gap in coil to allow line of sight for the IRtc.*

2.5.1.1. Sanity Check

In order to test the IRtc and the feasibility of this calibration test, a calibration was first run on the carbon plunger, which is a near black body (100% IR emission). The thermocouple was placed inside the plunger, half way between bottom and top. The RF coil was positioned so it covered

the top half of the plunger, and the IRtc was aimed directly below coil. Data collection proceeded as described above. Four tests were performed in succession, and then the testing apparatus was disassembled and the thermocouple changed. Four more tests were then performed.

2.5.2. Calibration Setup

Figure 12 shows the calibration test setup. The small chamber below the quartz tube was comprised of a thermocouple feed through at the bottom, spacers in the middle, and a compression fitting at the top providing a seal against the quartz. The thermocouple was wound around a ceramic rod for axial support and fit into the carbon plunger at the top. The IRtc was held in place by an adjustable arm fixture, attached directly to the machine, and positioned and aimed as previously specified. The BMG was placed on top of the carbon inside the quartz and then heated using the RF coil. A computer program was written to collect data from both the IRtc and the thermocouple. The data was collected at a rate of twenty points per second and recorded on a spreadsheet for analysis. The power output of the induction heater was held constant. Data was collected until the BMG reached a temperature of 1000°C, at which point the power was shut off, and the sample was left to cool. The tests were performed under a vacuum of 10^{-5} mbar.

2.5.3. Results

The tests revealed that the IRtc is accurate within 10°C. It was assumed that the thermocouple was accurate to the manufacturer's specifications, and this was observed in the lack of variation between the two thermocouples used. The discrepancy in the output signal of the IRtc (mV) could have been caused by background noise, which, despite filters on the output signal, is always present. The signal's rate of change was proportional to the heating rate of the BMG, which corresponded to a temperature difference between discrete points of ~1°C. It follows that a minor influence from background radiation would cause the IRtc signal to change, resulting in a perceived temperature change. Regardless, the trial proved that the instrument was capable of a calibration within an accuracy window acceptable for the process.

Once the calibration setup was proven in theory, the three calibration scenarios were run using the BMG. Unfortunately, none of these tests gave reproducible results. During testing, however, the likely causes of failure in calibration were observed. As the solid piece of BMG melts, it is not possible to control its position inside of the quartz tube. The distance from the sensor changes as the solid melts and sinks into the melt pool. This affects the emissivity, as the surface angle of the BMG relative to the IRtc is changing. Furthermore, once the entire sample is

molten, the electromagnetic waves created by the RF coil have a stirring effect on the melt pool. The melt can be seen spinning inside of the quartz tube. Because of this stirring, the emissivity of the liquid BMG is ever changing within the focal point of the IRtc, as hotter and cooler regions of the melt pool cycle through.

One way to overcome this problem would be to heat at a slower rate, or hold the temperature constant for even a few seconds. This would increase the sample size of data collected and allow for an effective average in determining the true temperature of the melt. The added time, however, allows the BMG to react with the quartz, effectively lowering the emissivity. The melt also reacts with the thermocouple shielding, eventually destroying the thermocouple. As it were, the thermocouples in this test were replaced every three to four runs because of corrosion. In the other two scenarios, where the thermocouple was embedded below the surface of the carbon plunger, different problematic phenomena were occurring. The RF coil couples (electro-magnetically) with the BMG but also with the carbon plunger. Factors, which effect coupling, include: weight, shape, and position of the BMG sample, position of the RF coil, size and density of the carbon plunger, and voltage of electricity passing through the coil. All of these, with the exception of the shape and position of the BMG, can be keep constant between test trials with careful attention. To ensure the shape of the solid remain constant, however, the BMG would have to be preformed or machined to size. This would also allow for more precise positioning within the quartz barrel and ensure that the entire sample of BMG resided inside of the coil at the beginning of heating. Sometimes the shape of the BMG was longer and narrow, which put a top section outside of the heating zone. The amount of BMG within the heating zone determines how well the coil couples with the BMG, as opposed to the carbon, which is nearby and highly conductive itself. This also presents a problem with measuring the temperature of the melt through the carbon, as the carbon is heated directly by the coil and at differing intensities depending on shape and size of the pre-cast BMG. Another problem, related to the inconsistent coupling and melting of the BMG, was the diffusion of heat across the 0.010" carbon to the thermocouple. Again, this is a problem due to the heating rate and short overall test times. The differences in melting cause inconsistent formation of the melt pool between runs. The faster the pool forms, the longer the melt has contact with the surface of the carbon plunger and the more time heat has to diffuse across to the thermocouple. This is the inherent problem observed in housing the thermocouple in a conductive material. The necessary heat conductivity brings with it the undesirable electrical conductivity. Certain materials do exist, sapphire for example, which were not explored due to cost constraints.

2.5.3.1. Conclusions from Calibration of the IRtc

Due to time constraints, further calibration approaches were not attempted. Instead, the data, which was collected with the thermocouple in direct contact with the melt, was reconsidered. The data was collected with respect to time, so the temperature with respect to time was known. Over the eight tests run, the temperature versus time data correlated within 20°C. The heating rate was dependant upon the power output of the induction heater, and this could be kept constant. Despite the problems discussed above, the data revealed a rough correlation between time and temperature, which held within 20°C above 600°C. For every second of heating, the temperature increased by approximately 100°C between 600°C and 1000°C. Fixing a time for heating, then, would give a fairly reproducible means of injecting at the desired temperature. Resorting to this method of melt temperature control was not ideal, but time prevented further investigation into calibration of the IRtc. Suggestions for remedy of the calibration problems have been included in chapter 7.

3. PROCEDURES

3.1. RF Coil

The radio frequency coils, which attach to the induction heater, are hand made from copper tubing. Water passes through the tubing and cools it during heating. Standard quarter inch (OD) copper tubing was bent around a cylinder that had a slightly larger diameter than the quartz tube. Kinking is an issue, and a winding diameter of 0.5 inch was the smallest achieved. Using a 3/16" (4.76 mm) diameter tubing when small coil diameters are desired helps this. A minimum of two complete turns is required for proper operation of the coil, which corresponds to roughly 13 mm in coil height at the minimum coil diameter. The 3/16" inch coil was filled with sand and capped on both ends in an effort to avoid kinks when bending. It was then wrapped around a half-inch (12.7 mm) cylinder to form the helical coil. After emptying the sand, the ends were sanded to prepare them for soldering. The ends were fit into the ID of quarter-inch tubing and soldered. The free ends of the quarter-inch tubing were then flared in order to mate with the compression fittings on the induction heater. Due to floor space constraints on machinery within the laboratory, the machine was located one meter from the induction heater, so the coil was that length and had an eighty-degree bend in it. Energy losses over this length were found to be negligible. Figure 4 shows the coil used in the calibration of the IRtc.

3.2. Mold Surface

The cavity side of the mold was left as machined. The other side, which was flat, was sanded and then polished on a wheel with five-micron aluminum oxide. The diamond tip of a micro-hardness indenter[22] was used to create pyramid-shaped indentations on the polished surface. The tip of the indenter formed an inclusive angle of ninety degrees, so the depth of the indentation was one half the length of a side. The tip of the indenter was less than one micron in width. A range of weights was used to vary the size of the indentation footprint. The smallest footprint was 10 μm on a side and the largest indentation was 150 μm. Seven different indentation sizes were marked

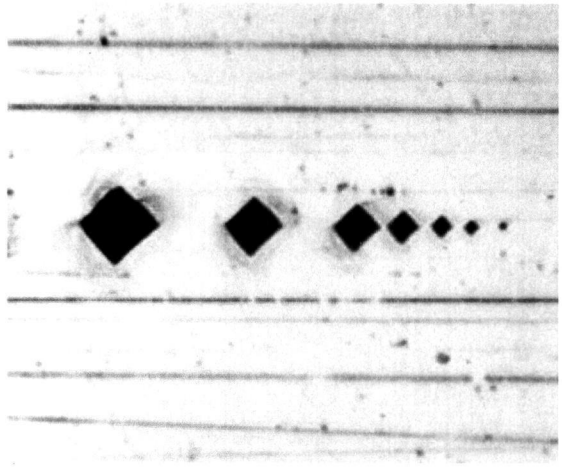

Figure 13. *Picture of copper mold surface and features created with a micro hardness indenter.*

into the mold in two groups; one near the gate, and one at the end of the cavity. The gradation can be seen in Figure 13.

3.3. Shot Size

The volume of the cavity of the first mold was 1.192 cm^3, which correlated to 7.1 grams of BMG. A diamond saw is used to cut the BMG to the desired shape and size. When possible, the number of pieces in the barrel is kept at two.

3.4. Running the Machine

All of the vacuum components are cleaned with 100% ethanol, as well as all of the items inside the chamber, which included the BMG sample, carbon plunger, mold, heaters, copper wire, quartz barrel, and support column. Size permitting, the components are cleaned using an ultrasonic bath of ethanol. Before cleaning, the quartz barrel is cut to size using a diamond saw to ensure a smooth cut surface. The quartz is placed into the slot in the mold and then sealed by tightening the clamping bolts. The cartridge heaters are connected to an electrical feed-through vacuum port using copper wire and copper connectors, crimped closed at the heaters and left as a slot fit at the feed-through pins. The heaters are first placed into the mold and then the mold is lowered into the vacuum chamber to rest on the quartz insulators, the quartz barrel passing through the compression fitting on the bottom flange of the chamber. The copper connectors are then fit onto the electrical feed-through pins. The support column is placed on top of the mold, and the top flange of the chamber is then tightened down. At the bottom of the chamber, the seal and compression fitting are tightened into place. The stand is then rolled into position and the RF coil placed around the outside of the barrel. Next, the BMG sample is loaded and the compression fitting between the injection cylinder and barrel tightened. The vacuum system connects to the chamber and pumps down to reach a vacuum of 10^{-5} mbar. The mold heaters are turned on and left to reach the desired temperature. Urethane hoses are used to connect the pressure tank to the valves and injection cylinder. The injection pressure is set to 90 psi [680 kPa]. The solenoid valve is connected to the data acquisition board and power supply. The induction heater is set at standby in preparation for control by the computer control program. The time limiting factor in set up was heating the mold, which took between 15 and 25 minutes depending on temperature. Once the mold temperature is reached, the control program is run. Starting the program switches on the induction heater. Once a melt temperature reaches 900°C, the solenoid valve is triggered, causing injection, and the induction heater is turned off. After the

injection, the chamber is filled with argon and left to cool in the inert atmosphere. Once cooled, the formed part is removed from the mold and the surfaces of the part and mold are examined with both an optical and scanning electron microscopes. For testing purposes, this process was repeated for mold temperatures between 200°C and 350°C at 25°C increments.

3.5. Vacuum System

A vacuum of approximately 10^{-5} mbar is achieved with the use of a turbo molecular pump[23] (TMP) backed by a roughing pump[24]. The chamber was not backfilled with an inert gas. The highest purity argon gas (for example) available is 99.999% pure. This correlates to ten parts per million (ppm) impurities, approximately twenty percent of which is oxygen. This leaves roughly two ppm oxygen in the chamber. Using the TMP, a vacuum of 10^{-5} mbar could be attained in the chamber, which leaves the same amount of oxygen in the chamber. The vacuum, however, essentially cleans the components inside of the chamber. The raised temperature of the components inside the chamber adds energy to the component material that aids in release of surface molecules. This was favorable because it effectively reduced the possibility for nucleation of the BMG by removing nucleation sites (any loose surface particles).

4. INITIAL RESULTS

4.1. Proof of Design

The initial testing of the machine was carried out before the mold heating had been finalized. The first injections, therefore, were into a mold at the ambient temperature of 22°C. There were problems encountered during the first few injections, but they will be addressed in the following sections. Nonetheless, the machine design was proven during these first injections with complete fill of the mold cavity. A picture of one of these can be seen in Figure 14. This shows the copper mold with the BMG part still in the cavity. The quartz barrel extends out from the cavity gate area. Figure 15 shows a picture of the BMG

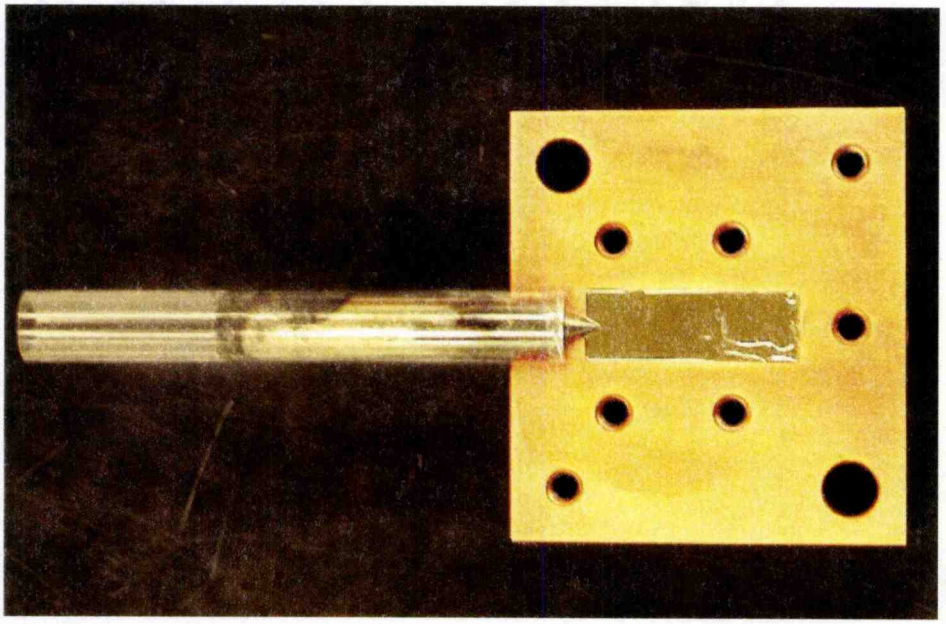

Figure 14. *Picture of complete fill from the initial validation of the machine design.*

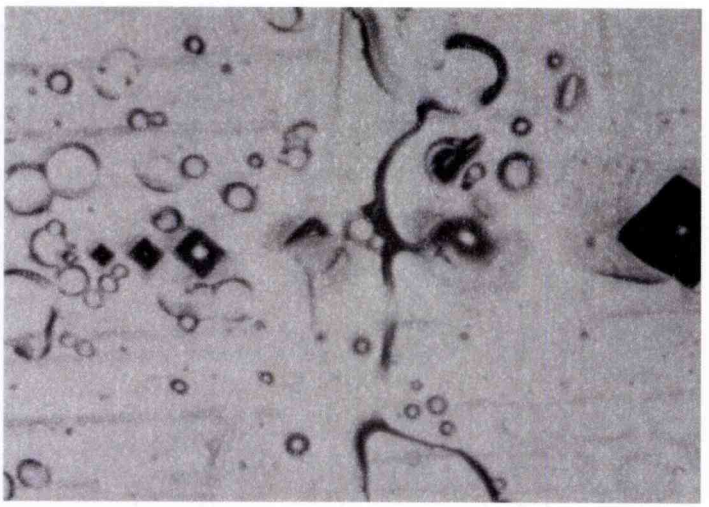

Figure 15. *Picture of the replicated mold surface showing partial replication of the indentations in the BMG.*

surface under an optical magnification of 400x. Figure 16 shows one of the indentations reproduced in the BMG. This picture was taken with a SEM at a magnification of 800x.

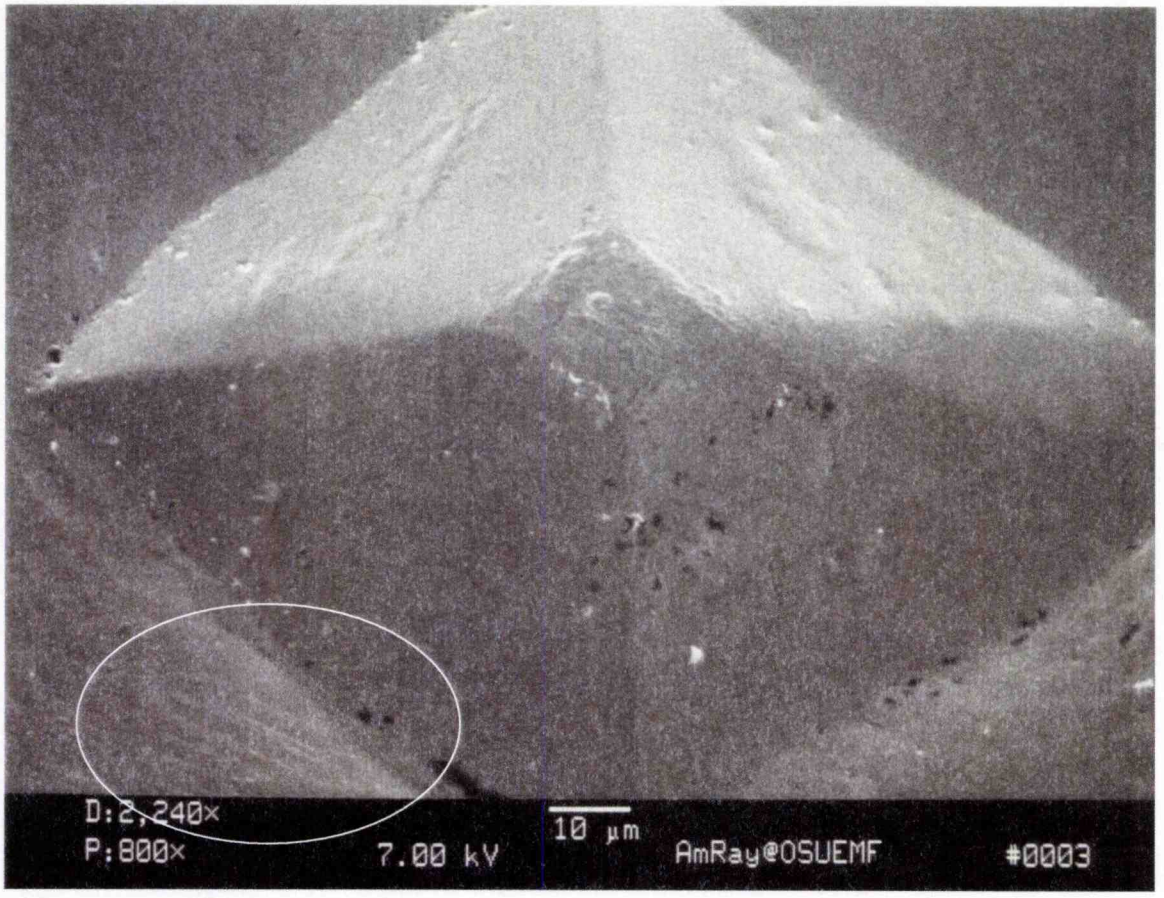

Figure 16. *Picture of BMG. Shear bands were created in the copper by the diamond indenter. The circled area shows the bands, replicated in the BMG. The melt froze before entire fill of the indentation.*

4.2. Discussion

Figure 16 is of particular interest because it gives an indication as to the replication capabilities of the BMG. The shear bands, created in the copper by the indenter, have been replicated. These ridges of the bands are less than one micron in width. The tip of the pyramid is also less than one micron (not shown), but it has not filled (shown in Figure 16). The melt cooled before reaching the point of the indentation. The shear bands indicate the ability of the BMG to replicate sub-micron features, but this replication is dependent upon the rate at which heat is removed from the melt. It would seem, then, that a higher mold temperature would cause the melt to cool more slowly, allowing the melt to fill the pyramid completely.

Figure 15 is a picture of the indentations as replicated by the BMG. Some of the indentations have not replicated, while indentations on both sides have. A likely explanation for this result lies with the turbulent filling of the mold. The uneven flow over the surface would create a difference of velocities and could have an effect at this scale. The unfilled indentations may be the result of the turbulent flow front. This is discussed further in section 5.2.1.

5. MACHINE REDESIGN AND FINAL PROCEDURES

As with any machine design, there were several problems encountered during the trial runs. What follows is a list of some problems that warranted redesign in some fashion in order to improve upon the original design.

- Measurement of the melt temperature was not accomplished with the IRtc, rather an empirical time-temperature relation was be used.
- The gate design was altered to promote more even filling.
- The injection pressure was increased from 90 to 140 psi.
- The plunger and barrel were resized and the plunger and cylinder rod interface reworked.
- Inserts were added to the flat side of the mold, and the micro features were placed on these inserts instead of directly onto the mold.
- The RF coil shape was modified to address the wetting of the BMG to the quartz.
- The chamber was backfilled with 99.999% argon.

A detailed discussion of these changes follows.

5.1. Melt Temperature

Calibration of the IRtc to the BMG was not successful. A detailed discussion of these efforts can be found in section 2.5. The result of the calibration tests was to change from temperature measurement in real time to empirical measurements of the temperature that correlate to the heating time.

5.2. Filling

The gate into the cavity was merely a conical extension of the barrel cylinder. It was located in the center of the thick region and had a diameter of 3.18 mm, which was the entire thickness of the part wall. The size of the gate was kept large in order to facilitate with filling, more specifically, to avoid freeze off. The surface of the part reveals that the filling of the cavity was uneven. Figure 17 is a picture of the BMG part, and the surface lines indicate that the first melt to enter the cavity traveled down the middle of the cavity and froze without touching the sidewalls. The rest of the melt, then, proceeded to fill in around this frozen section, which acted as an inhibitor to further jetting. The flow of the melt was diverted to the sides of the cavity, allowing the rest of the part to fill. The effect on surface finish can be seen. This phenomenon is known as jetting in the plastics injection industry and is often the result of poor gate placement or design.

5.2.1. Discussion of Filling

Ideally, the melt front would not separate during filling. A continuous flow front during filling would ensure that any given cross section along the length of the mold contacted the mold surface at relatively the temperature. When jetting occurs, the melt, which fills around the already frozen

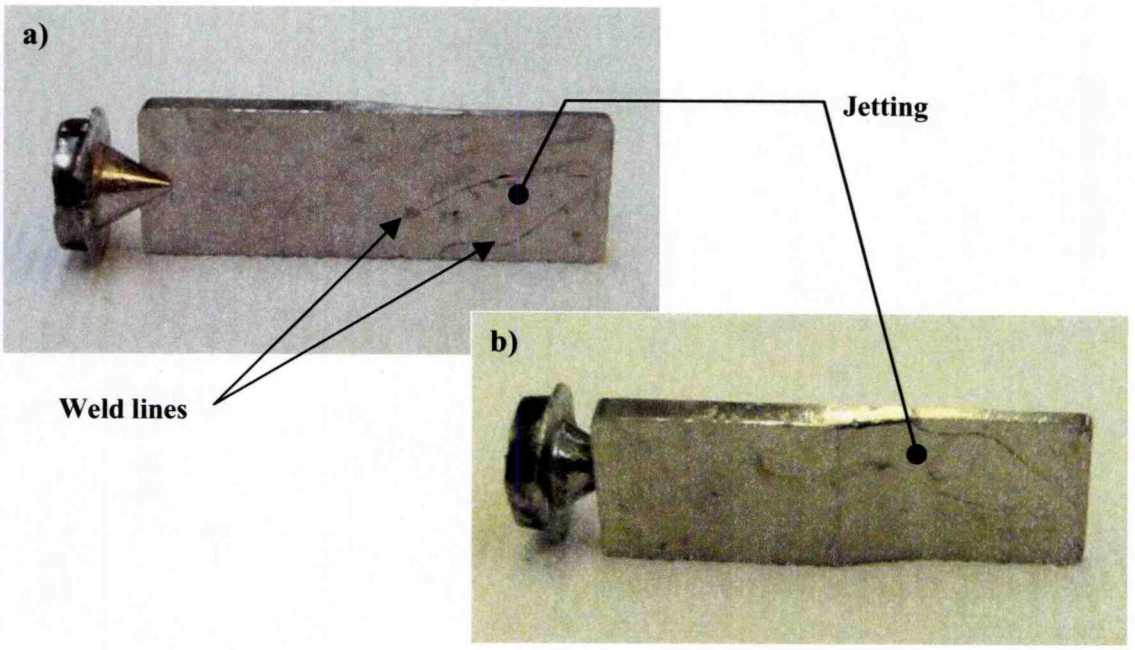

Figure 17. *Pictures of a BMG part which show the evidence of "jetting" on both the (a) flat and (b) cavity side of the part.*

portion, is cooler and of a higher viscosity. This gives inconsistent information about surface replication, as the jetting phenomenon is not a controllable factor. In an effort to create a more uniform flow front, a mold with a lap-style gate[25] was built. The difference between the first mold and this design can be seen in Figure 18. This gate is machined into only one side of the mold and shuts off against the other half at the parting line. The melt enters the gate, which redirects the flow by ninety degrees, causing the melt to hit the cavity surface before continuing on to the end of fill. This seeming obstruction to filling is intended to create a puddle of material, which will then expand to fill the mold. This can be seen in Figure 19, which is a picture of short-shot (caused by a cracked barrel) injection through a lap gate. The surface tension of the expanding puddle keeps the melt front together.

Filling, then, is dependant upon balancing the injection pressure with the viscosity of the melt, which is a function of time, melt temperature, and mold temperature. The filling rate should

be fast enough to prevent the viscosity from becoming so great that complete filling is prevented. If, however, the rate is too fast, the flow front becomes unstable, which leads to flow front separation and poor surface replication.

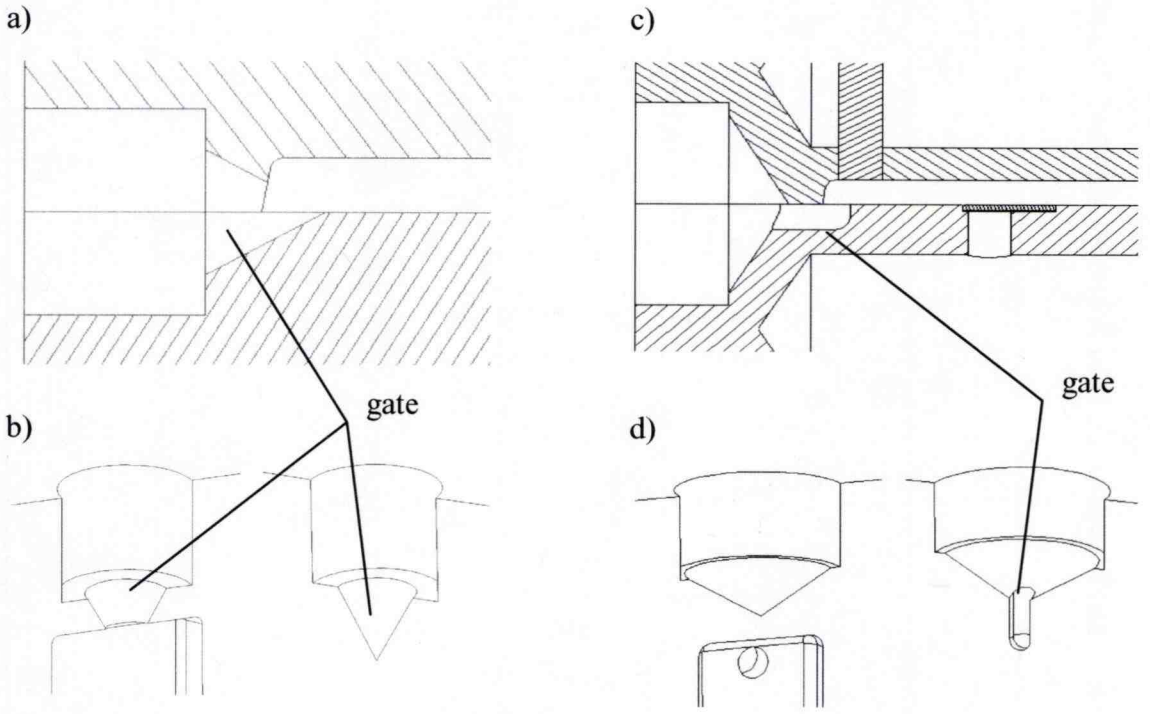

Figure 18. *A schematic diagram of (a) cross section view of the gate area and (b) isometric view of each mold half of Mold Rev 1. Mold Rev 2 is a "lap"-style gate, which is also shown in (c) cross section and (d) isometric views.*

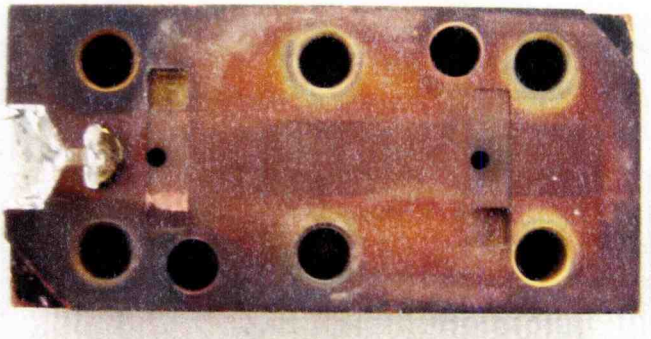

Figure 19. *A picture of the flow front created by a lap gate.*

The lap gate design resulted in an even flow front, but the gate was prone to freeze off during injection, so that the cavity did not fill completely. Figure 20 shows a picture of a linear flow front on an incomplete fill. The frozen material ahead of the flow front is most likely the result of the melt splashing when first entering the cavity. The melt, which followed in filling, had a lower viscosity. The puddle-like appearance of the filled section is evidence of the gate's influence on filling. Even so, the small gate (1.59 mm) removed heat from the melt too quickly at the gate region. The gate size was then increased to 3.18 mm, and Figure 21 shows the result. The fill is more complete, but the melt still froze at the gate. After several failed attempts at complete fill, the gate size was increased again by extending it across the parting line into the other mold half. This gave a direct line of travel from the barrel into the cavity. The cavity now filled completely on a consistent basis. This is shown in chapter 6.

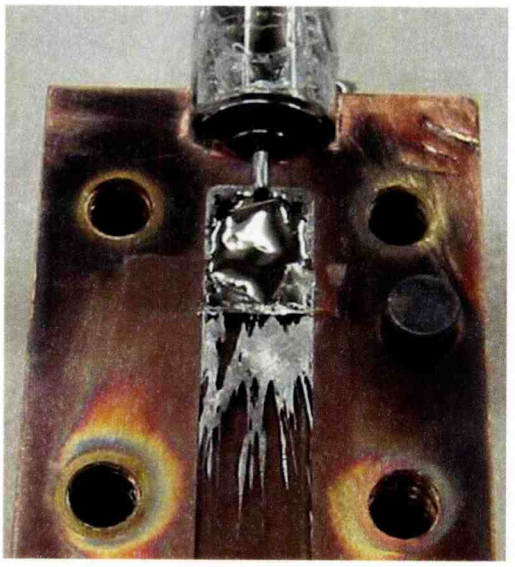

Figure 20. *Picture of incomplete filling showing linear flow front. The initial splash of the melt as it entered the cavity at high velocity is seen here.*

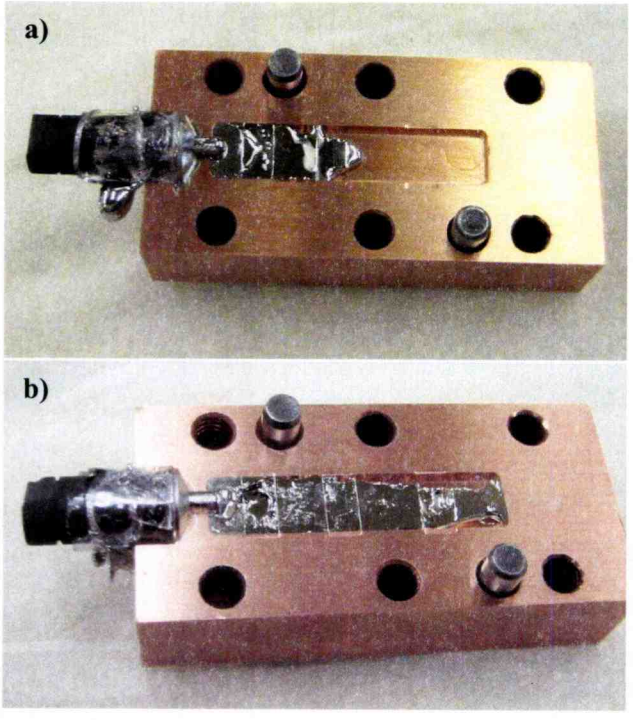

Figure 21. *(a) Picture of incomplete fill with larger lap gate at a mold temperature of 250°C. (b) Same mold and gate, still showing incomplete fill at a mold temperature of 300°C.*

5.3. Vacuum

Several injections resulted in a loss of vacuum in the chamber. This happened when the quartz tube cracked, or a seal failed, allowing air to enter and react with the melt. Oxygen reacted with the melt causing crystallization upon cooling. When the melt crystallized, the BMG had a tendency to stick to the mold. A picture of one such case can be seen in Figure 22. The picture of the cavity shows a region, running the length of the cavity, which experienced a chemical bond. The ridges on the surface of the BMG indicate that this may have been the first of the melt to enter the cavity, like the jetting effect described previously.

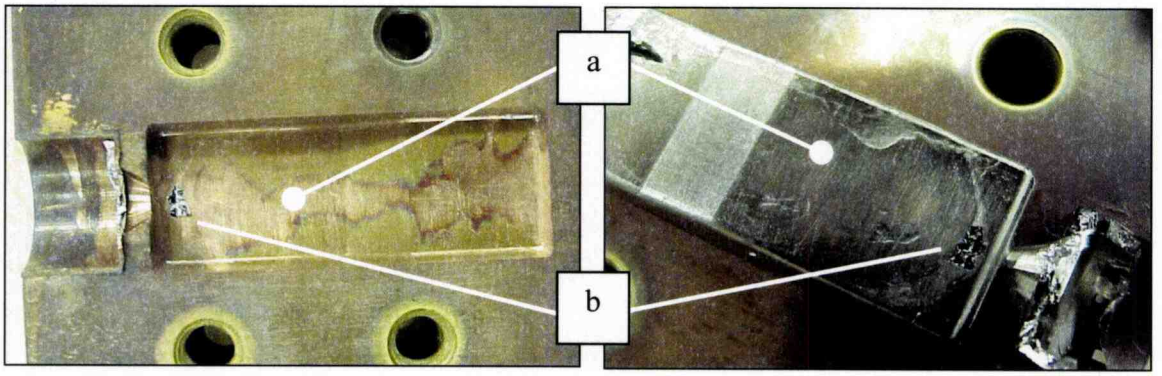

Figure 22 *Pictures of mold and molding that were exposed to oxygen at a mold temperature of 375°C. (a) Evidence of jetting effect. (b) The alloy has crystallized, which makes it brittle. Part of the molding has broken off and stuck to the mold.*

The remedy for the cracked quartz is discussed in the following section. The failure of the Viton seal occurred at the interface of the barrel and vacuum chamber. During heating, the RF coil coupled with the compression port, which heated the port and ultimately melted the seal. A simple solution to this would have been to move the injection assembly down, away from the seal, so that the heating zone would be far enough away. Doing so, however, would increase the distance the melt had to travel from the heating zone to the cavity. Instead, heating shields were placed between the RF coil and the port. This prevented the port from heating up, but the shields melted during heating. The final solution can be seen in Figure 23 on the following page. A cooling manifold was added onto the compression port. Water from a chiller was used to cool the port during heating. The cooling allowed the RF coil to be placed within six millimeters of the port.

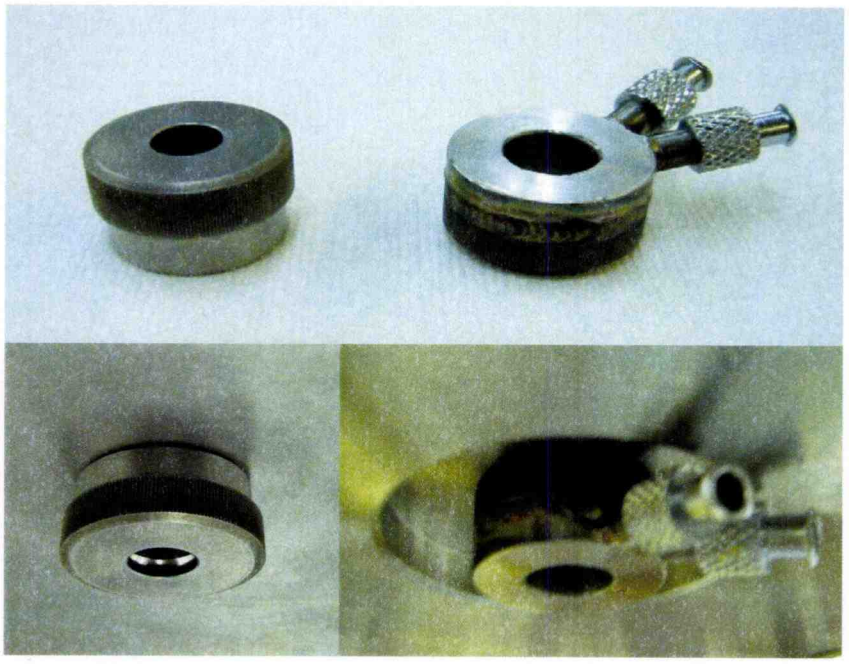

Figure 23. *Picture of compression port that provided a vacuum seal between the vacuum chamber and the quartz barrel. The port on the right has been reduced in height, and a cooling manifold has been welded on.*

5.4. Barrel and Plunger

The outer diameter of the quartz barrel was 9.5 mm. The inner diameter was 7.5 mm. This diameter was sized slightly larger than the cylinder rod, which extended through the barrel. The machine was designed with careful attention given to alignment of the injection cylinder and vacuum chamber, but misalignment of the injection cylinder of even one degree would result in stresses being transferred to the quartz cylinder during injection. This may have been the reason the quartz barrel cracked during some of the injections.

The interface of the cylinder rod and the carbon plunger was a sliding fit. This was changed to allow for the possibility of misalignment of the injection cylinder. The top of the cylinder rod was formed into a dome shape, and the plunger was changed to a simple cylinder. If the

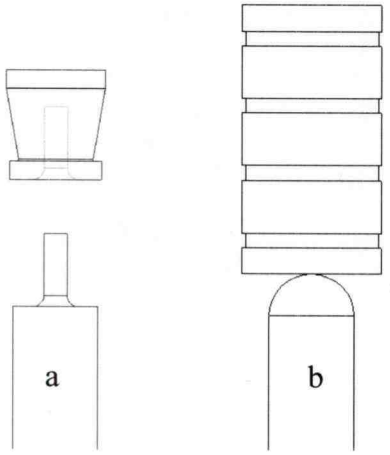

Figure 24. *2-D image showing (a) design I and (b) design II of plunger and cylinder rod.*

cylinder was misaligned, the dome could slide across the flat bottom side of the plunger while maintaining full injection pressure. Because the cylinder rod could not be reduced in diameter, the quartz tube was increased to the next standard size of 0.5 inch OD. This allowed for ample clearance between the two. See Figure 24 above.

5.5. Surface Features

The pyramid shapes created by the micro-hardness indenter were made on the flat side of the mold. If the injection process failed, or the mold needed to be cleaned, frequently the surface would need to be refinished. This meant polishing again and adding more indentations. This process was time consuming, so mold inserts were considered. First, silicon wafers were used in an effort to avoid polishing altogether. The wafers were too brittle to survive an indentation, but a laser could be used to cut holes, or lines. Figure 26(b) shows a picture of a cut made by the laser in the silicone. Lines were even more desirable because they would give an indication as to how feature orientation, relative to flow, affected fill of the feature. Small cavities were machined into the flat side of the mold for the inserts. The length of an insert extended beyond the cavity walls on the opposite mold half to provide the shutoff when the mold was closed. The clamping force of the mold held the insert in place during injection. Unfortunately, the silicon bonded to the copper once the temperature was raised to operating temperatures, and the brittleness of the silicon made it difficult to work with. Next, stainless steel and oxygen-free copper inserts were made. To save on preparation time, the stock material was machined so that

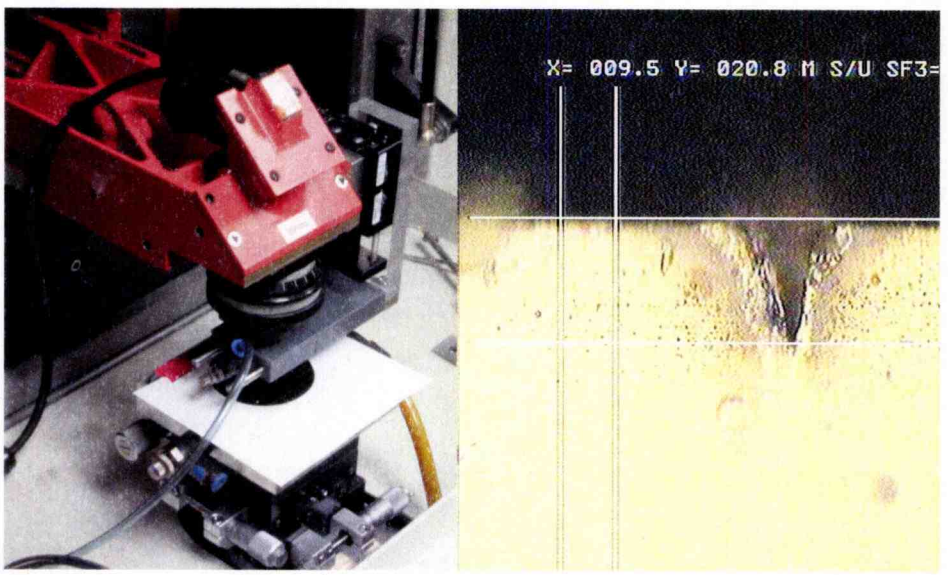

Figure 26. *(a) Picture of Laser scribing setup. (b) Picture of scribed silicone wafer showing the cross section of a line feature. The width (x) and depth (y) are shown in microns.*

multiple inserts could be made at the same time. After sanding and polishing, the block of material was attached directly to a diamond saw and the inserts were cut off at a thickness of 0.040 inch, as seen in Figure 26. After this, the insert was placed on a stage and a diamond-tipped scribing tool was used to create lines with a V-shaped cross section. These lines were oriented with and across the direction of melt fill. Figure 27 shows a picture of the scribing device and inserts which have been scribed. The reflecting light makes the scribe easily visible.

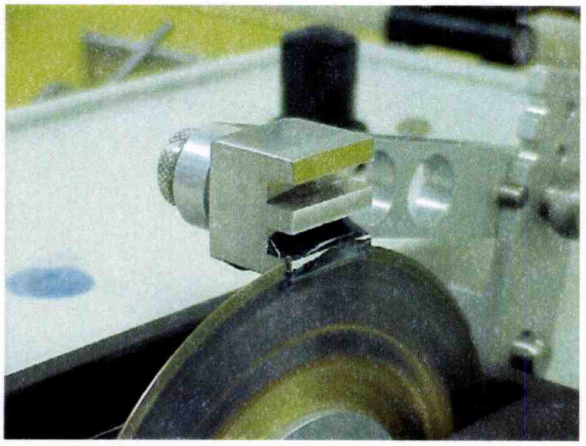

Figure 26. *Picture of polished stainless steel insert cut to size using a diamond saw.*

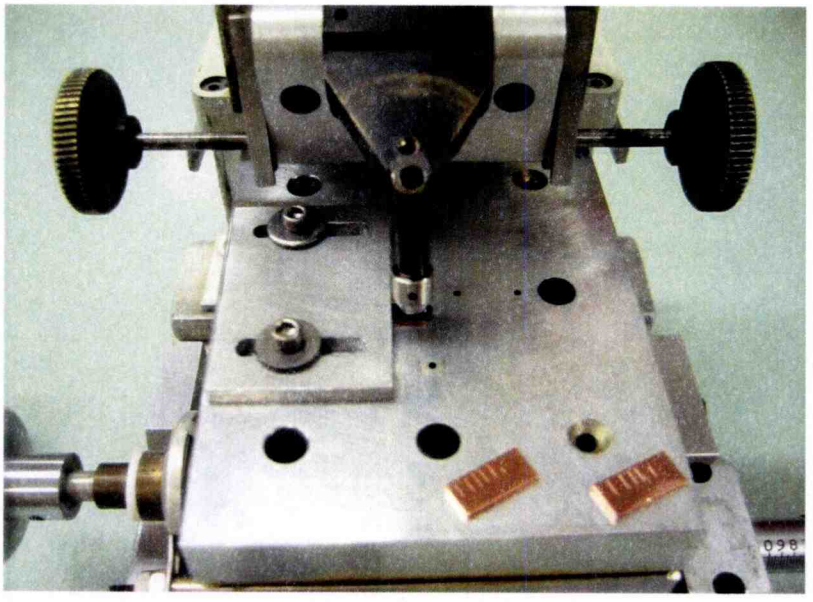

Figure 27. *Picture of the scribing device and two copper inserts which have been scribed.*

5.6. Wetting and Climbing of the Melt

The melt had a tendency to climb out of the heat zone during heating. Once the melt reacted with quartz, the reactive layer promoted wetting and allowed the melt to progressively travel up the barrel wall and out of the heating zone. This was a problem because the material outside of the heating zone would then cool and prevent the plunger from pushing the melt into the mold. To correct this issue, a helical coil was used to create a field gradient, as seen in Figure 28. This caused the shape of the melt pool to also take on a cone shape within the quartz, so that the upper half of the melt pool was no longer in contact with the quartz during heating. The magnetic field counteracted the climbing effect and resolved the issue.

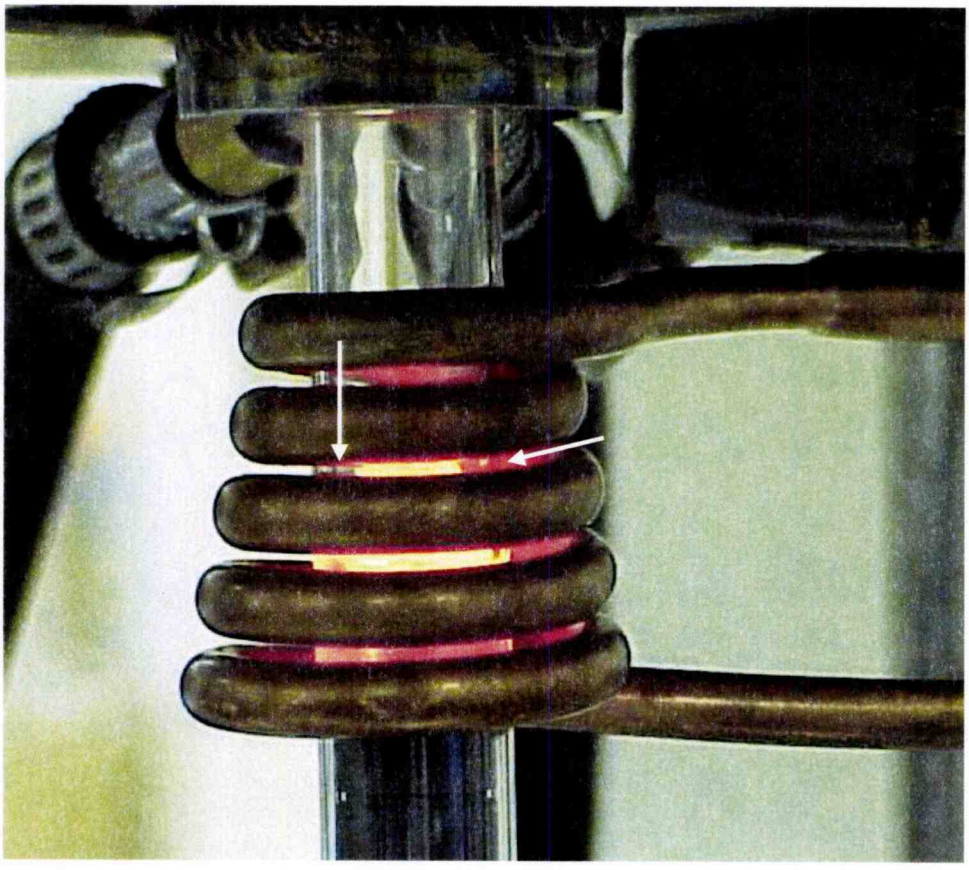

Figure 28. *Picture of conical coil showing the effect of the coil shape on the molten BMG. The BMG is kept from the quartz barrel along the upper half of the pool.*

6. Final Results

After the modifications to the machine were completed, the success rate increased from approximately fifty to ninety percent, with regards to complete cavity fill. Several pictures of these moldings follow. The best feature replication was observed when stainless steel inserts were used, as opposed to the copper. Sub-micron sized features were, however, replicated in both the copper and stainless steel. There did not seem to be any correlation between filling of the feature and its orientation relative to flow. Surface energy effects are present during filling. A picture of a typical casting can be seen below in Figure 29.

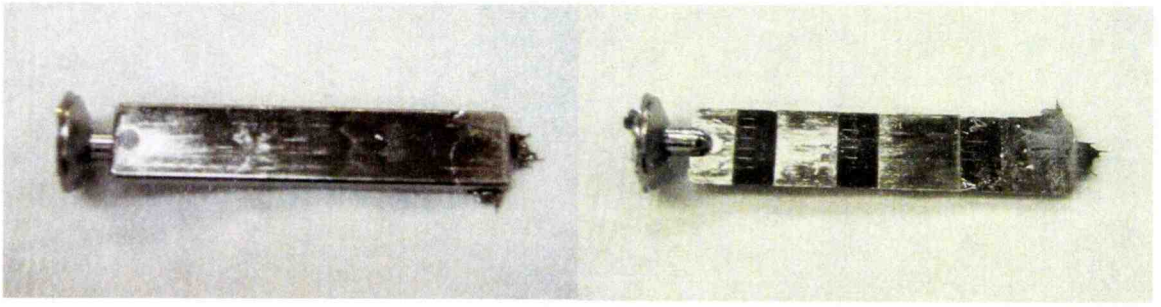

Figure 29. *Picture of BMG showing complete fill. The flash is a result of the melt entering into the vents at the end of fill.*

6.1. Replication of Stainless Steel Surface

Figure 30 on the following page shows pictures taken with an optical microscope of features replicated in the BMG. The melt temperature was 950°C, the mold temperature was 275°C, and the chamber was backfilled with argon to atmospheric pressure. Figure 30 also shows pictures taken with a SEM of both the BMG and the mold insert. The width and depth of the scribed feature is 30 μm and 18 μm respectively. Notice the tip of the feature, which has filled completely. Furthermore, at the base of the feature, the surface of the insert was replicated, and sub-micron replication can be seen here. The two sets of arrows point to noticeable features on the insert and BMG cast part. Note that the magnification is slightly different between the two photos. To verify the BMG did in fact replicate the surface, a backscattered image of the casting was taken with the SEM. The lack of shade contrast on the surface of the BMG indicates that the material surface is in fact homogenous. The image is shown in Figure 31. The darker regions are merely shadows created by the tilt angle of the sample inside the SEM. Had there been contrast, it would have revealed the presence of some material other than BMG (perhaps some of the mold surface) at the surface of the casting.

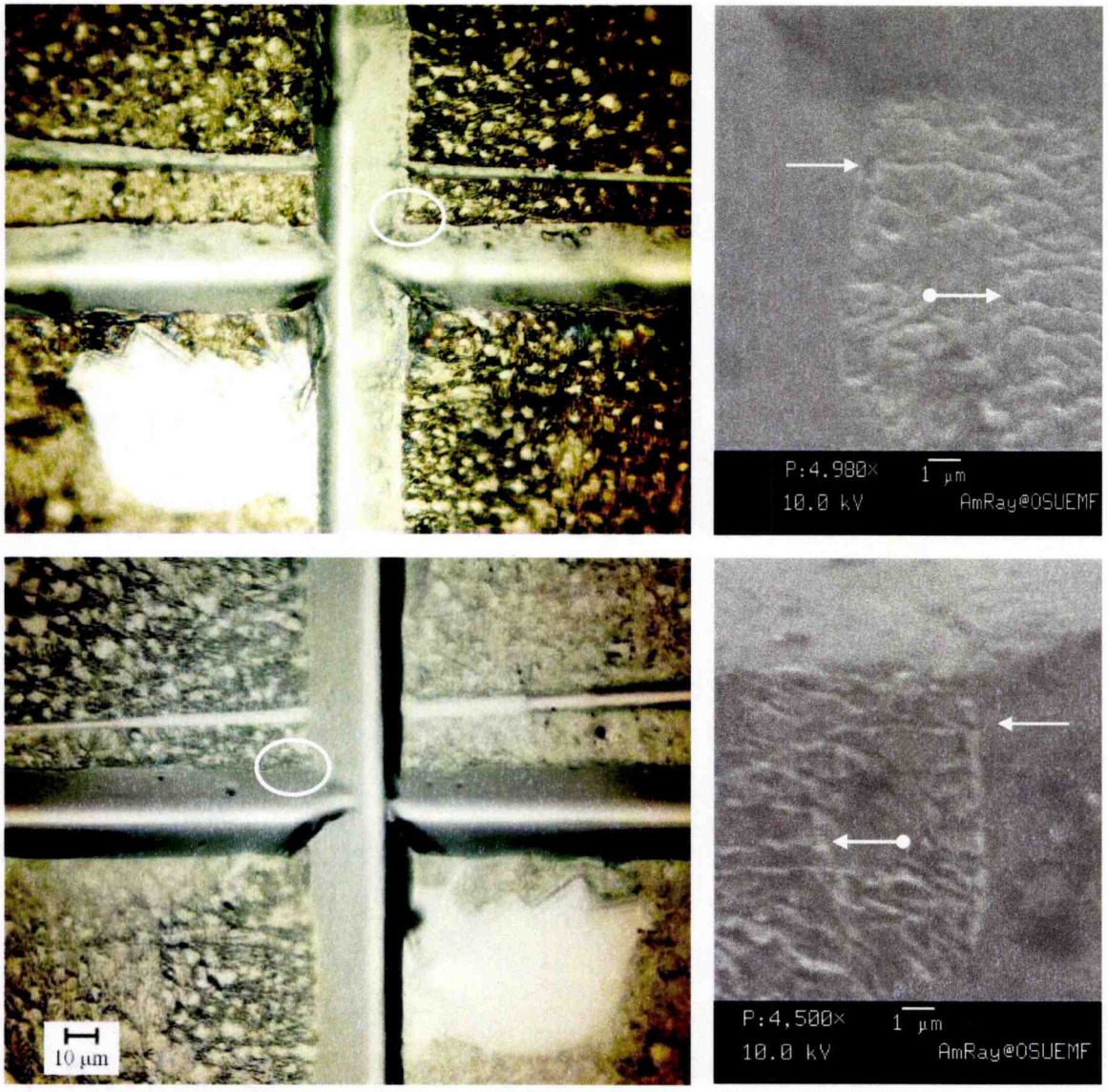

Figure 30. *The photos above were taken of a bulk metallic glass (BMG) casting, which was formed in a copper mold. The top two photos show the surface of a stainless steel insert that was placed into the mold; the bottom two are of BMG. The photos on the left were taken with an optical microscope at 400x. The photos on the right were taken with an SEM and the magnification is indicated. The casting shows that replication is possible to a sub-micron scale. Arrows indicate two easily noticeable feature areas that were replicated.*

6.2. Replication of Copper Surfaces

The mold surfaces, with the exception of the inserts, were left as machined. The surfaces were cleaned with ethanol after each use but were otherwise left exposed to air. The inserts were

polished, scribed, and cleaned in an ultrasonic cleaner before each use. Figure 29 shows a BMG part molded at a mold temperature of 275°C. Macroscopically, the fill appears excellent. The SEM, however, reveals that the mold features have not actually filled, only the outline of the features are replicated. Figure 32 is a SEM photo of the BMG surface in contact with the copper inserts. The surface is very smooth, except at the edges of the features, where the melt wetted slightly (seen macroscopically). The photos of the BMG parts made for each mold temperature between 200°C and 350°C are nearly identical. None of the parts showed replication of the features on the inserts. The other surfaces of the mold, however, showed better replication. Figure 33 shows pictures of the mold surface at the transition between the barrel and the gate. Here, the BMG has replicated the surface down to the micron level. Figure 34 shows an optical photo, and one taken with the SEM, of the cavity surface of the mold at the end of fill. The region, which is circled, appears to have different reflectivity to light. Closer examination revealed that this area replicated the mold

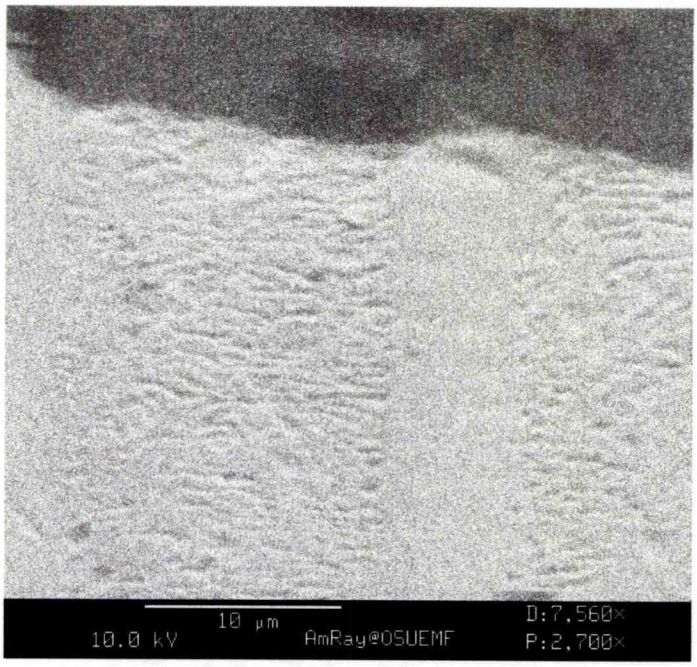

Figure 31. Backscattered image taken with a SEM to verify that the casting surface was a homogenous replication of the steel insert. The darker areas are shadows.

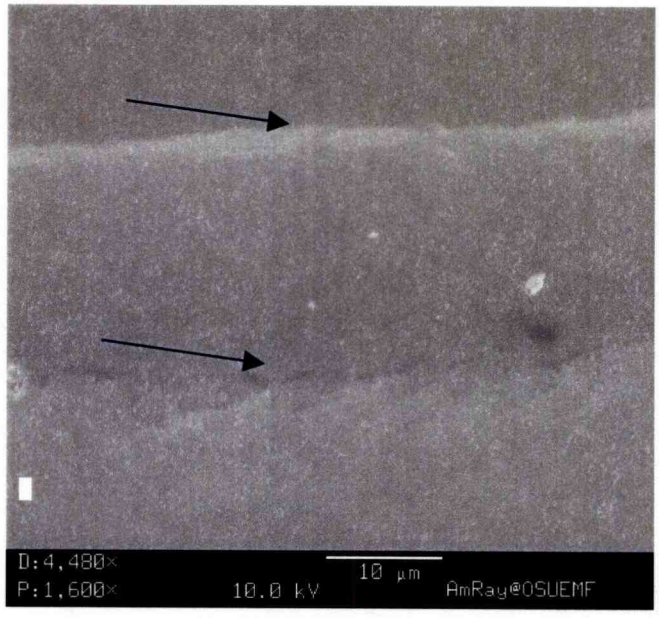

Figure 32. *SEM photograph of BMG replication of a copper insert in an argon atmosphere. The arrows indicate the edges of the scribing the copper.*

surface down to the sub-micron size.

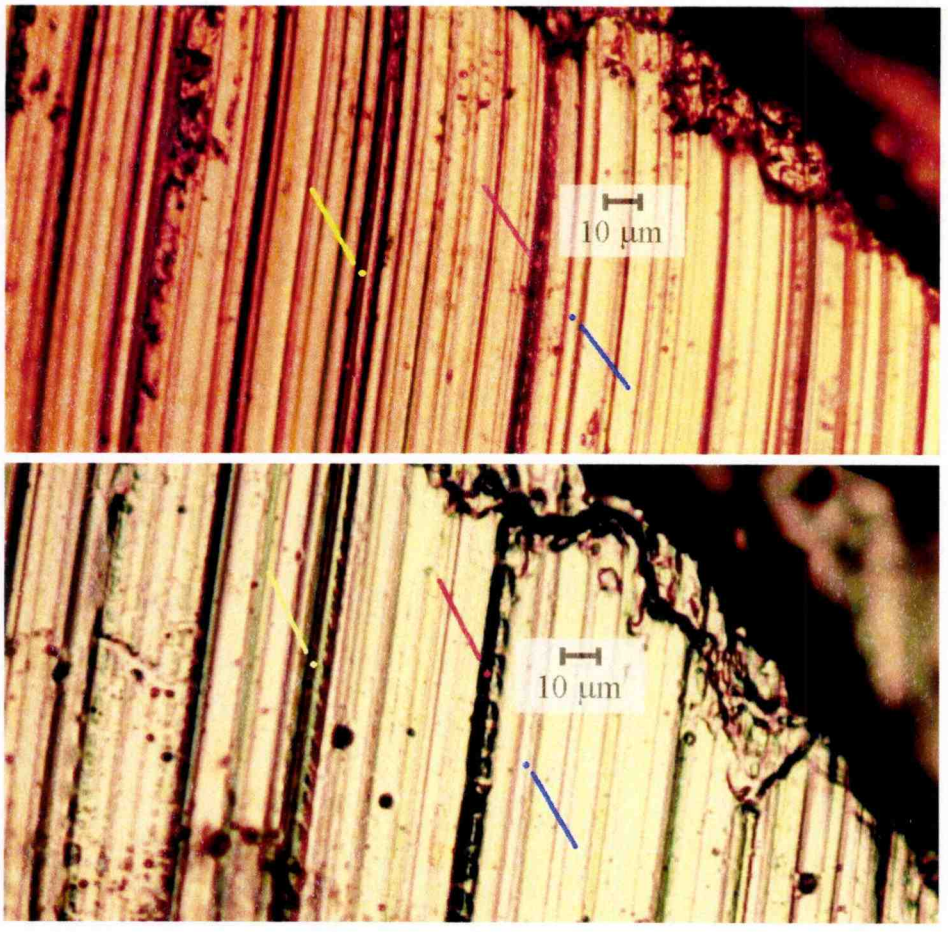

Figure 33. *(a) Picture of machine marks above the gate area on the copper mold. The mold temperature was 275°C during injection in an argon atmosphere. (b) The BMG is shown to replicate in the copper down to micron size.*

The rest of the surface around this area did not replicate as well as the area shown in Figure 34. Figure 35 shows a different BMG casting, which has a gap at the end of fill in the same relative location as the region that replicated well on the part shown in Figure 34. Gaps and voids did occur in several of the BMG parts. They were observed when the vents, located at the end of fill, became blocked by cooled melt that reached the end of fill before the rest of the part had filled. It may be that the argon gas, which was trapped at the end of fill, was super-heated by the melt pressure during the injection shown in Figure 34. In plastics injection molding this is known as a "gas trap." When the cavity is not properly vented, trapped air is compressed and super-heated, so that the plastic is burned by the gas. In the case of a metal, the melt would not be burnt, but it may experience a temperature spike, which would lower the viscosity and

promote surface replication. It is also possible that an oxide layer is burning off, or degassing with the local increase in temperature.

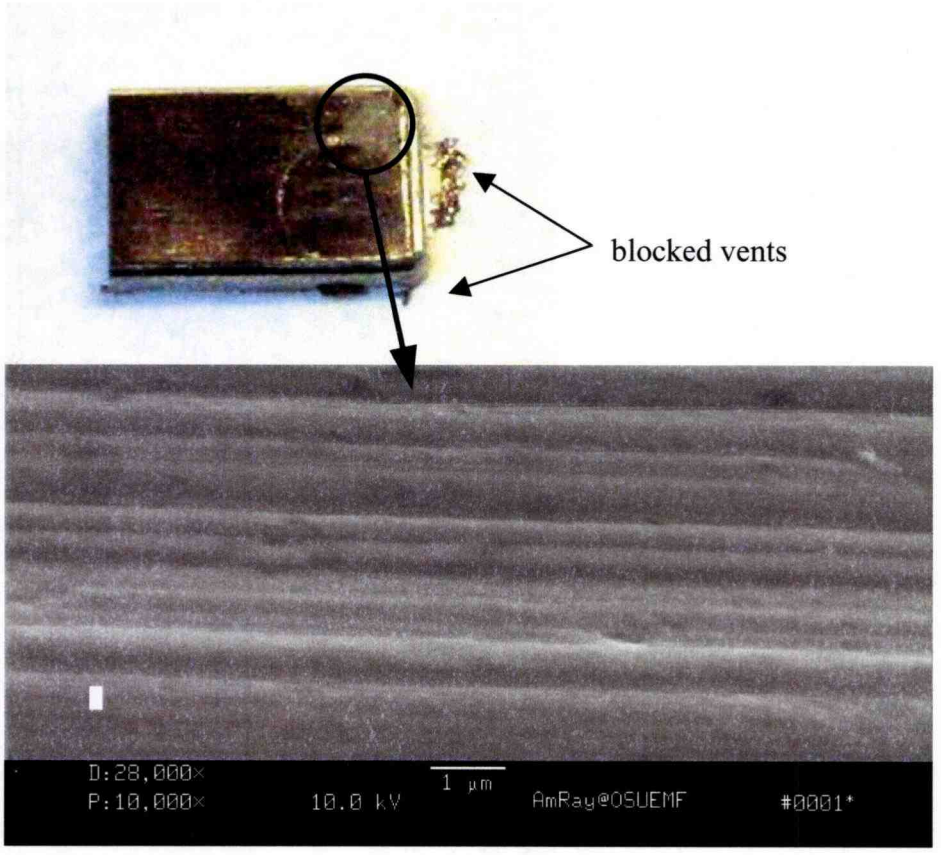

Figure 34. *(a) Picture of the end of a cast BMG part cast in a copper mold. The circled area appears "blushed," and (b) a SEM photo of this area reveals excellent replication of the copper surface in this area, as compared to the areas adjacent.*

Figure 35. *Photo of the end of fill showing a gas-trap region. This was a common occurrence when the chamber was backfilled with argon gas. Venting the mold differently would prevent this void.*

6.3. The Effect of Surface Energy

It appears that the presence of the inert gas discourages wetting of the BMG to the copper and quartz. Under vacuum, the BMG melt wetted to the inside of the barrel during injection, so that a thin film of BMG remained on the inside surface as the plunger pushed the melt into the mold. When argon was present, no wetting outside of the heat zone occurred. No film from the melt was left behind on the barrel wall after injection, which can be seen in Figure 36. It was also observed that the melt cast in an inert atmosphere did not fill the features in the copper inserts in any reproducible manner. Additionally, as mentioned in the previous section, mold temperature did not have a noticeable effect on feature replication. Figure 37 shows examples of preferential wetting to the machined surfaces, rather than the polished copper inserts. The stainless steel inserts, however, had a tendency to stick to the BMG after cooling. Some of these parts stuck to the stainless inserts due to local crystallization, a result of the poor thermal conductivity of the stainless steel.

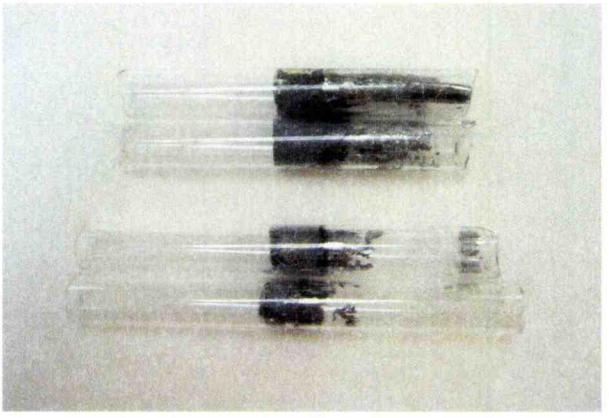

Figure 36. *(a) The quartz barrel after injection under high vacuum has a layer of metallic glass left behind by the plunger. (b) In an argon atmosphere, there is no wetting of the metallic glass to the quartz surface. It is supposed that surface energies are responsible for this.*

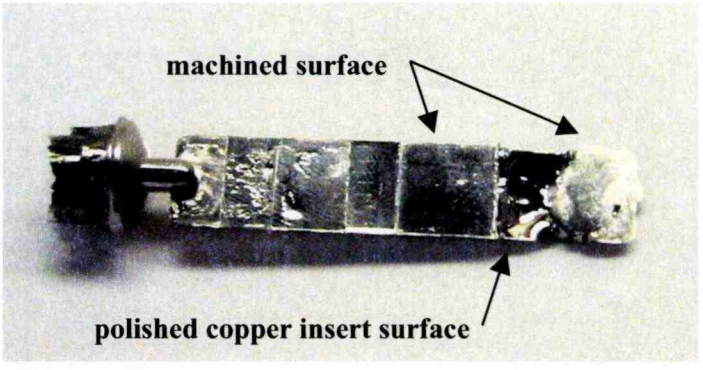

Figure 37. *Photo showing preferential wetting of the BMG to the machined surface of the copper mold, as opposed to the polished copper insert surface.*

7. FINAL DISCUSSION AND FUTURE CONSIDERATIONS

7.1. Vary Melt Temperature

It is recommended that a thorough investigation be carried out on how surface feature replication is affected by the temperature of the melt. It is further recommended that melt temperature be studied in conjunction with mold temperature and other significant processing variables, such as injection speed, to account for interactions. A design of experiments (DOE) study would help determine the relative effect each process variable has on feature replication.

7.2. Melt-delivery System

The injection speed of the machine is dependant upon the pressure of the gas used to drive the injection cylinder. Varying the pressure at which the injection occurs will change the speed at which the melt enters the mold. As built, the machine is not capable of a quantitative study on injection speed, but qualitative analysis is possible. Two areas of interest may be: the critical speed to avoid gate freeze-off, and a short-shot filling analysis. By injecting a smaller volume of material, the flow front would not reach the end of cavity. Observing the frozen flow front would give an indication of filling turbulence. To quantitatively analyze the injection speed, a Hall-effect sensor may be attached to the outside of the injection cylinder. By adding a small magnet to the aluminum piston ring inside of the cylinder body, the position as a function of time could be detected by the sensor and recorded by the same program that triggers the injection.

Profiling the injection speed and pressure is another avenue to explore. Ideally, the melt would leave the heat zone very quickly and travel to the gate in minimal time to avoid heat loss. Once at the gate, however, the speed should be reduced because the melt experiences a large pressure drop through the gate. This pressure drop slows the injection but not before some material passes through the gate at a much greater speed. A similar effect is known in plastics injection molding as "jetting," which was discussed earlier in section 5.2. A stream of material enters the mold cavity before a flow front is established. This stream cools before the rest of the melt, so that the remaining molten material flows in and around the cooled material, raising concerns of material inter-bonding and part homogeneity. Profiling the injection speed may promote an even flow front and less turbulent filling. Further recommendations for filling are discussed in the next section (7.3).

A hydraulic injection system would be better suited to the casting process because of the compressibility of gas. Using hydraulics would enable a slow speed with high pressures,

something not possible with the gas cylinders, where compressibility prevents a constant pressure at slower speeds. The system, however, would also require an accumulator to allow for rapid injection or larger pressures. The hydraulic system was not used in the original design because of cost constraints.

7.3. Gate Study

The shape and size of the gate affects how the melt enters the mold and how quickly heat is removed at the gate region. Both the tab and lap gates were attempted in the machine qualification. Lap gates of 3.18 mm and 1.59 mm diameter both experienced freeze off and incomplete filling. It is recommended that a modified fan gate be implemented. This gate would provide a smooth transition between the circular barrel end and the linear part edge. Flow originating from a line, rather than a point, should promote an even flow front and help prevent the observed jetting effect. To accomplish this study, the gate region of the mold may be constructed as an insert to allow for multiple design trials. Incomplete fill at various injection speeds would give a good indication of the effect the gate has on filling because the flow front could be observed. A fast injection may have an inertial effect on the melt, so that the flow front reaches the end of the cavity and freezes with more material at the end opposite the gate. Conversely, slower injection speeds should be used to study the shape with complete fill of the cavity behind the flow front. The slower speeds may require a larger gate to prevent freeze off, but most likely higher injection pressures would be sufficient. For future manufacturing purposes, it would be desirable to keep the gate as small as possible to allow for removal.

7.4. Wetting of the Melt and Mold Surfaces

7.4.1. Injection Atmosphere

Complete fill of the mold cavity was possible under high vacuum and when backfilled with argon gas, but replication of the features in the polished copper was possible only under high vacuum. It would be beneficial to understand the effect of the inert gas on wetting. A study in which the chamber is backfilled with inert gas to several pressures less than one atmosphere may give some insight on the matter. It may also be of interest to look into inert gases other than argon. These studies should be quantified by characterizing the replication of the mold or mold insert surfaces.

7.4.2. Surface Energy

In addition to the injection atmosphere, the surface finish of the mold should be considered, preferably in the same study. There was a noticeable difference in how the BMG wets to the polished and machined surfaces, as discussed in section 6.3, and the scribed lines also show a tendency to promote wetting. A study in which the surface finishes of the inserts are varied from a polished to coarse finish may provide information on how surface energy affects wetting and, consequently, filling. Specifically, the surface replication would be compared, as it is possible that affecting the surface energy will affect the tendency of the melt to travel into small crevasses, such as the micro-scribed features. Another study may look at the effect of directional scribe channels, shallow or deep, which may influence the direction or shape of the flow front. Because the melt was observed to wet out at sharp radii, a series of micro-sized notches along the edges of the cavity walls, for example, may promote wetting and result in a more even flow front as well. The mold material should also be considered in a future study, as the surface energies for each metal are different. Steel, stainless steel, and copper have been used, but they have not yet been quantitatively compared.

7.5. Venting

If the injection happens in an inert atmosphere, venting is needed. The vents added to the molds during the machine qualification were a best guess, based on die-casting and plastics injection mold design practices. Some of the parts produced showed flash in the vent areas, and some showed evidence of trapped gas in the cavity (see section 6.3). In the latter case, the flow front often reached the end of fill and blocked the vents before the mold could fill completely. This resulted in voids and incomplete fill of the cavity. Placement, dimension, and frequency of the vents may be a useful investigation.

7.6. Surface Features

If features other than dots or lines are required, it is recommended that laser machining be further investigated. Under the right conditions, a laser can remove stainless steel via an ablation process. The shape of the beam is parabolic, making it an ideal cut in terms of mold release. This process was discussed in section 5.5.

7.7. Flow Length and Critical Thickness

Designing a study to characterize a critical flow length of the BMG is recommended. Such a comparative test is employed by the plastics industry and the results provide a simple comparison of filling capabilities between plastic resins. The test would require a mold with a flow path length sufficiently long so as never to be filled completely. A spiral flow path is commonly used, having a rectangular cross section. Such a cavity would not require a gate; rather the barrel would end perpendicular to the beginning of the cavity surface in the mold. Quantitative viscosity information would also be available from such a test, using capillary-viscosity calculations.

A wedge-shaped cavity may be used to determine the critical thickness of a particular BMG. Filling from thick to thin with no gate, the barrel would end at the beginning of the cavity on the thick end. After cooling, the cast part would be cut in cross sections of varying thickness and checked for evidence of crystallization (using a differential scanning calorimeter for example). The greatest thickness, which reveals no signs of crystallization, is the critical thickness. This would also be a function of filling rate, mold temperature, and melt temperature, and these values would have to be fixed.

7.8. IRtc Recommendations

A possible remedy to calibrating the IRtc lies in the shape of the RF coil. The tests were carried out with a cylindrical coil, as described previously. But, a conical coil was also used in the machine validation process. When the injection was carried out under vacuum, the melt had a tendency to climb the barrel walls, up and out of the heating zone, which was believed to be caused by wetting, or surface energy of the melt. To avoid this, a helical coil was used to create a field gradient, as discussed in section 5.6. A conical coil, then, could be made with a "window" in the coil that would allow the IRtc have a line of sight into the barrel at the top half of the melt pool. The emissivity would change only as a function of melt position, as the melt was observed to move violently in the conical field. The IRtc output, however, could be filtered through a statistical analysis program to give more accurate data. The main advantage with this coil would be the ability to avoid the reaction with the quartz barrel that affects emissivity. The melt would still react with the thermocouple housing at the bottom of the melt pool, but such a setup should give reproducible data output from the IRtc.

Another option would require a large amount of redesign. Essentially, locating the injection barrel inside of the vacuum chamber would negate the need for a vacuum seal between the mold and the barrel. If this were the case, the barrel could be made out of carbon, or another

material that has a lower reactivity with the BMG than quartz. If the barrel were carbon, however, the BMG would be heated secondhand, as the RF coil would couple with the barrel over the BMG. The IRtc could be placed inside of the chamber, or outside, if a sight glass were installed on the chamber. The focal point would be through the coil and onto the barrel surface. Simple calculations of heat transfer could be made to determine the temperature of the BMG inside of the barrel. Again, this type of design was not undertaken at the outset due to the high costs of more complex chamber and custom machined barrels, which have to be replaced after each shot. That said; it is very reasonable to assume that such a design would give reproducible calibration results and, therefore, allow for use of the IRtc during normal operation of the machine.

8. CONCLUSIONS

Replication of sub-micron features in bulk metallic glass is possible from the melt state using a die-casting process. The machine design has been verified by the successful casting of BMG parts. The processing variables that affect feature replication include, but may not be limited to: melt temperature, mold temperature, injection speed and pressure, injection atmosphere, mold material, cavity surface finish, and gate design. Further testing will be required in order to quantify, or at least make relativistic comparisons of, the variables that affect the ability of the BMG to replicate a cavity surface. The capacity to process a metallic glass from the melt state with low pressure and low temperatures has also been demonstrated. It is foreseeable that further development in these areas will lead to the ability to manufacture well-defined, extremely small, features on the surface of die-cast BMG parts.

BIBLIOGRAPHY

1. H.A. Bruck, *Scripta Met. Mat.* **30**, p.429 [1994].
2. W. Clement, R.H. Willens, and P. Duwez, *Nature* **187**, p. 869 [1960].
3. A.L. Drehman, A.L. Greer, and D. Turnbull, *Appl. Phys. Lett.* **41**, p. 716 [1982].
4. H.W. Kui, A.L. Greer, and D. Turnbull, *Appl. Phys. Lett.* **45**, p. 615 [1984].
5. R.B. Schwartz, R.R. Petrich, and C.K. Shaw, *J. Non-crys. Sol.* **1976**, p. 201 [1985].
6. A. Peker and W.L. Johnson, US Pat. No. 5,288,344 (February 1994); A. Peker PhD dissertation, California Institute of Technology, 1994.
7. W.L. Johnson, *MRS Bulletin/October*, p. 43 [1999].
8. A. Inoue, T. Nakamura, N. Nishiyama, and T. Masumoto, *Mater. Trans. JIM* **34**, p. 351 [1993].
9. Ibid. 6, p.47, 54.
10. J. Schroers, C. Veazey, W.L. Johnson, *Appl. Phys. Lett.* **82**, p. 370 [2002].
11. Die Tech Industries LTD, Providence, RI.
12. Graphite rod stock. POCO, part #AXF-5Q
13. Fused quartz. G.E. type 214
14. Oxygen Free High Conductivity Copper. TMX, Thyssen Division
15. LSS 15 kW/200kHz Induction Heating Power Supply. Lepel Corp.
16. Micro Air® (3/4" bore, 3" stroke). Ingersoll-Rand, ARO
17. 24V DC Solenoid valve. SMC, part #VZ3140
18. 24V DC Power Supply. Power-One
19. 120V/20Amp Variable Autotransformer. Powerstat
20. Infrared Thermocouple. Exergen Corp., model# IRtc.4ALF-LO-E
21. GE quartz, http://www.gequartz.com/en/optical.htm
22. Hardness tester. LECO, model #M 400-A

23. Turbo Molecular Drag Pump. Pfeiffer Vacuum Inc., model# TMH071

24. Rotary Vane Pump. Pfeiffer Vacuum Inc., DUO 2.5

25. For a better understanding of some common gate types used in the plastics industry, refer to *Plastic Part Design*, R. Malloy, Haasen Pub., p.15, 1994.